Lecture 7. Vision and movement. 13.11.24

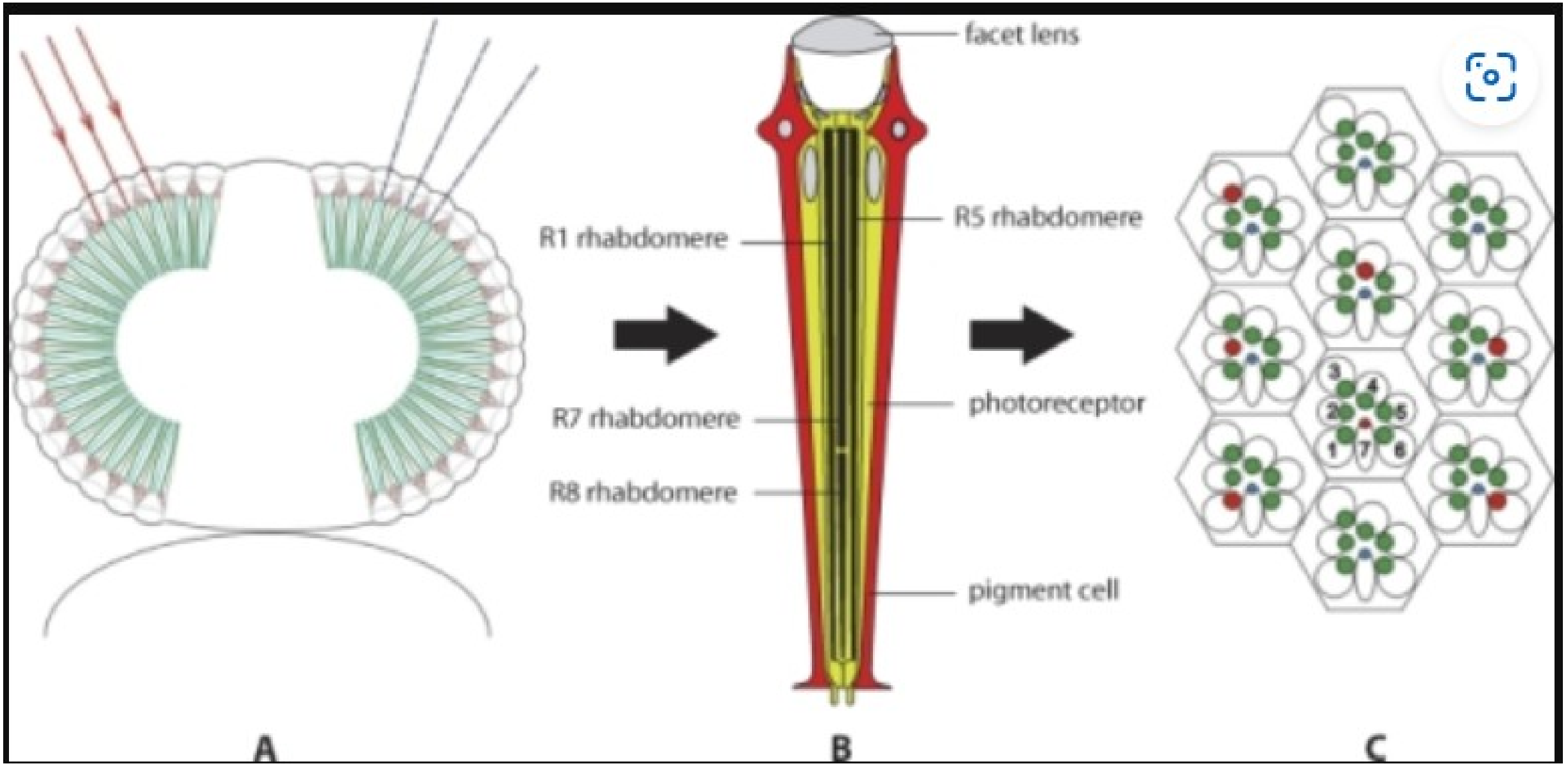
facet lens
R1 rhabdomere
R5 rhabdomere
R7 rhabdomere
photoreceptor
R8 rhabdomere
pigment cell
3
4
2
5
1
7
8
A
B
C

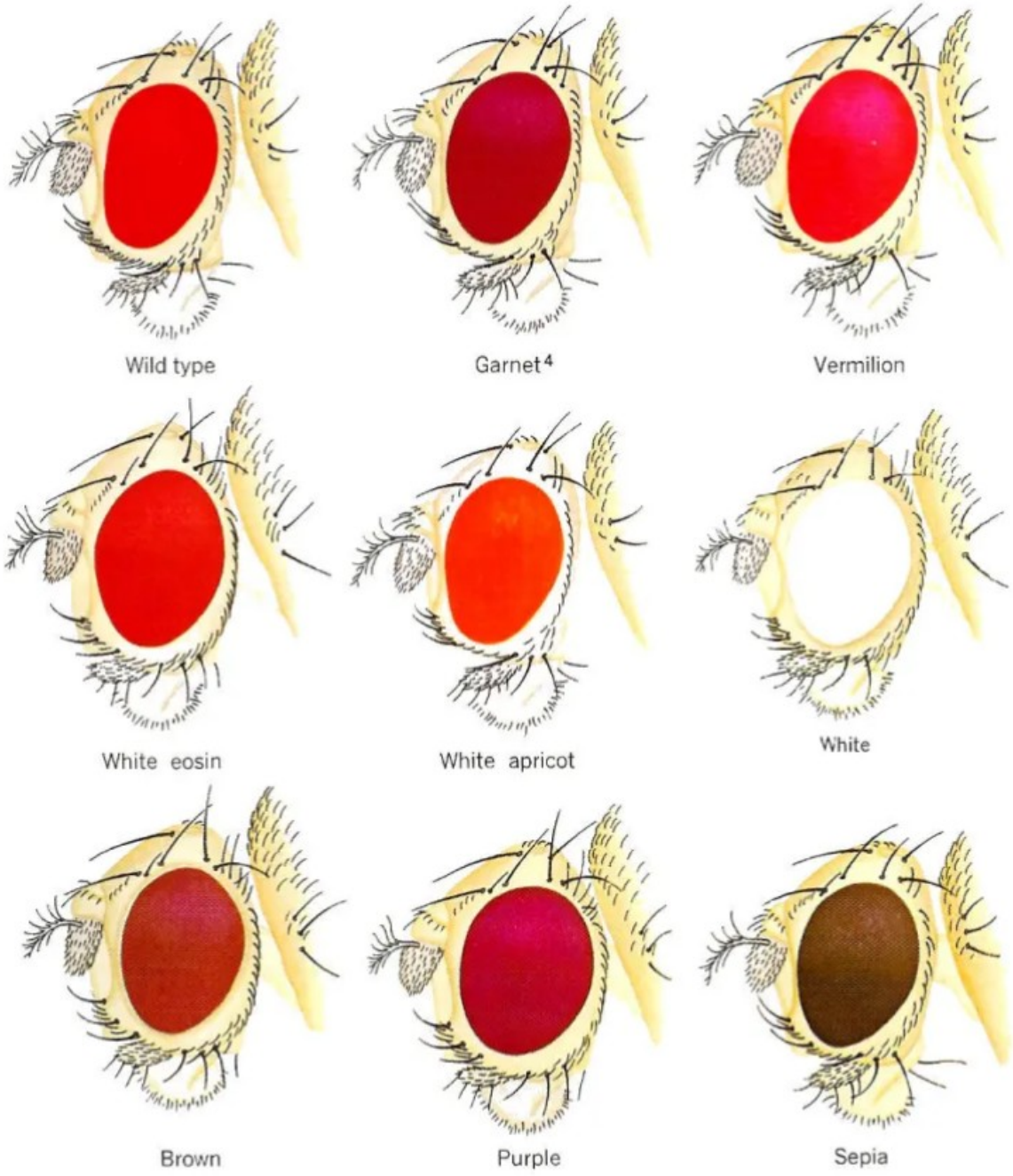

Plate I. *Some eye colors in* Drosophila melanogaster. *(After E. M. Wallace, in* An Introduction to Genetics *by Sturtevant and Beadle, Saunders, 1938.)*

Pigments are in lysosome-related organelles.

Fly eye colour genes are homologous to human albinism genes

Gary Larson cartoon.

This is not how a fly sees.

Visual neural superposition corrects for this

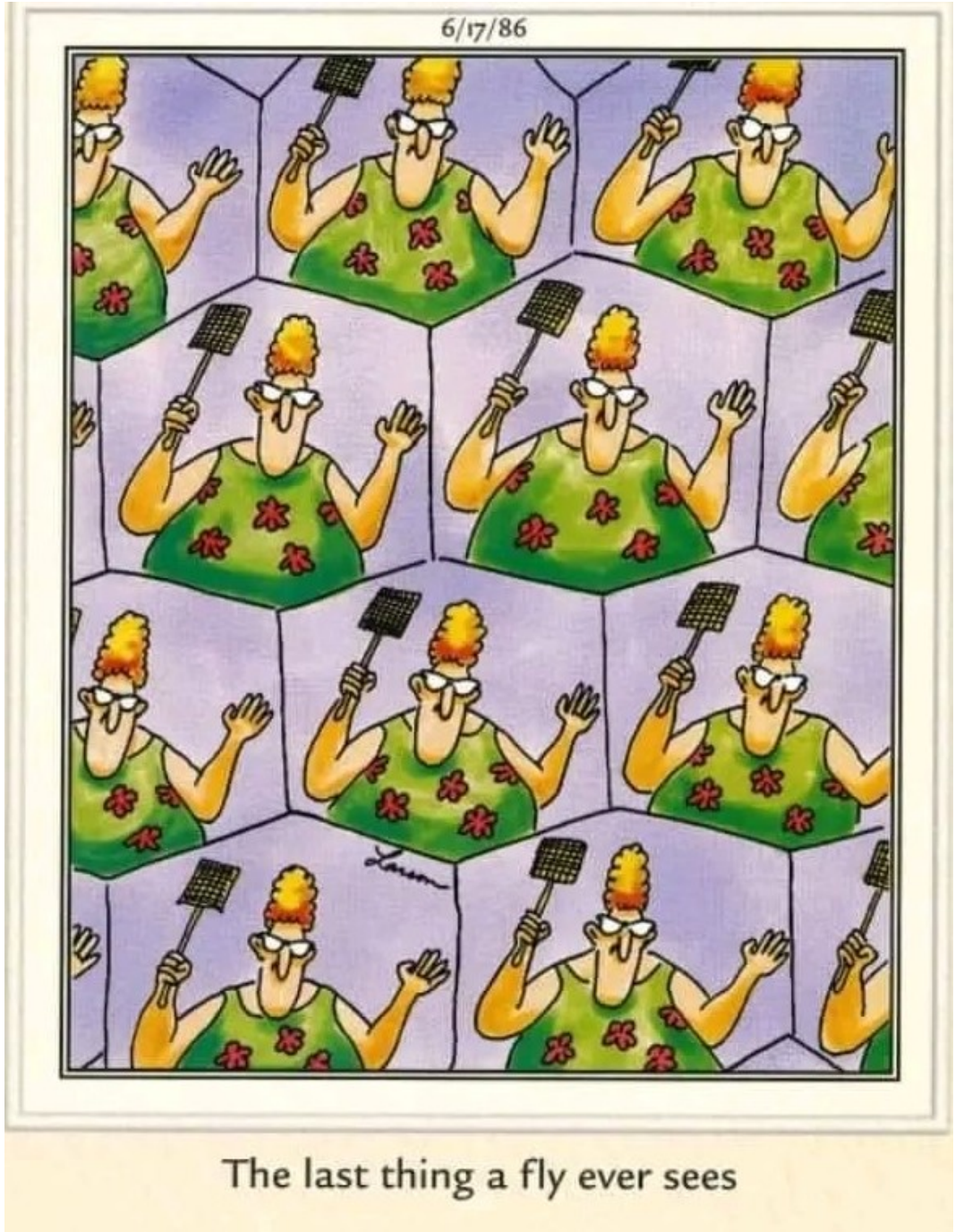

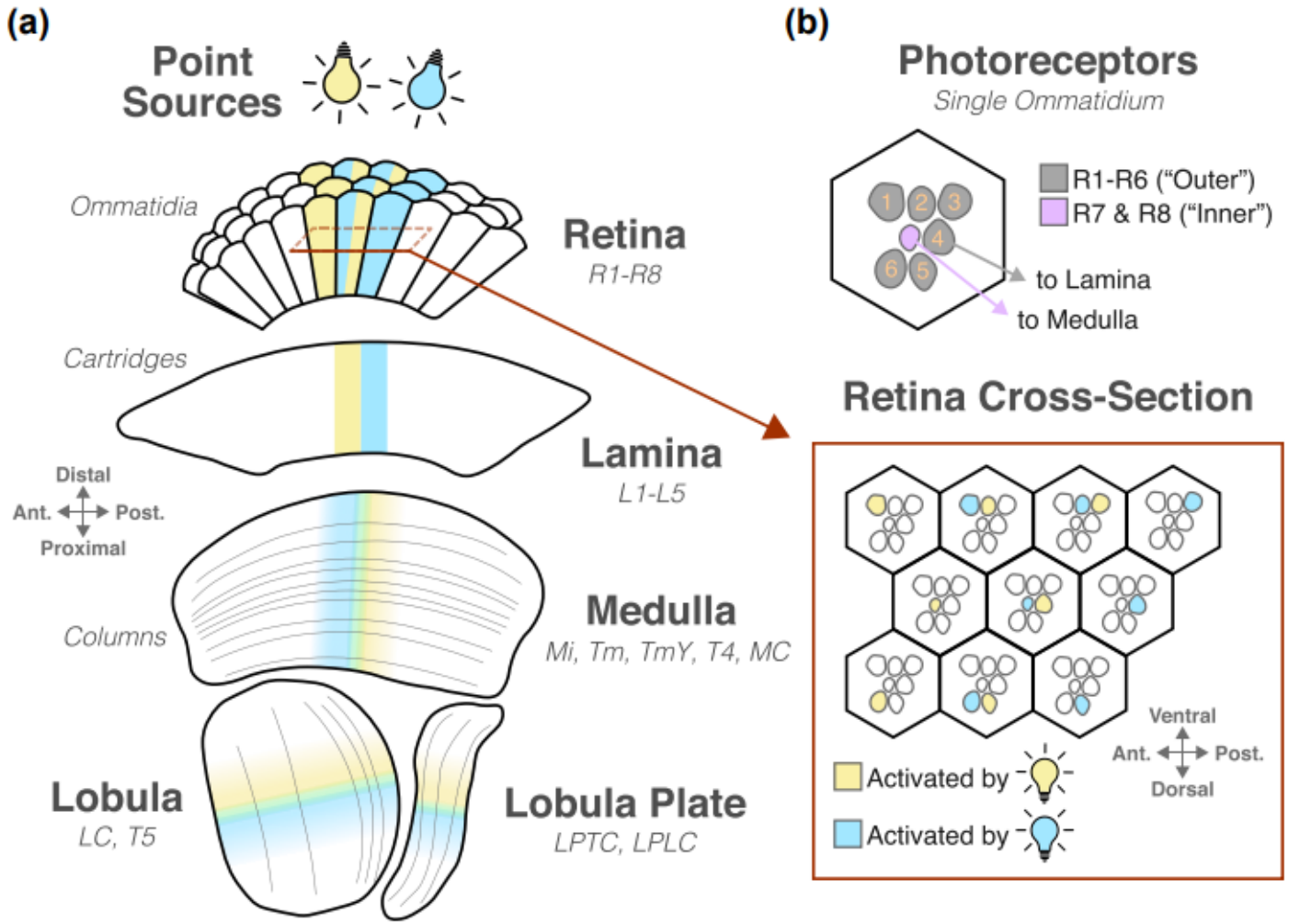

Fig. 2. a) Overview of the compound eye and visual system anatomy. A simplified horizontal section through the optic lobe shows the organization of the early visual system. The portions of each neuropil that are activated by 2 adjacent point sources of light are highlighted in blue and yellow. Green indicates a mixing of signals from both sources. Red box indicates the location of the retinal cross-section shown in b). For regions with prominent laminar organization, layers are shown as thin gray lines. The primary feedforward cell types are listed for each neuropil. b) Top: a simplified cross-section through a single ommatidium shows the spatial arrangement of individual photoreceptors. Bottom: "Superposition" is illustrated in a cross-section through the retina, as indicated by the red box in a). The pattern of photoreceptors that respond to the blue and yellow point sources is shown.

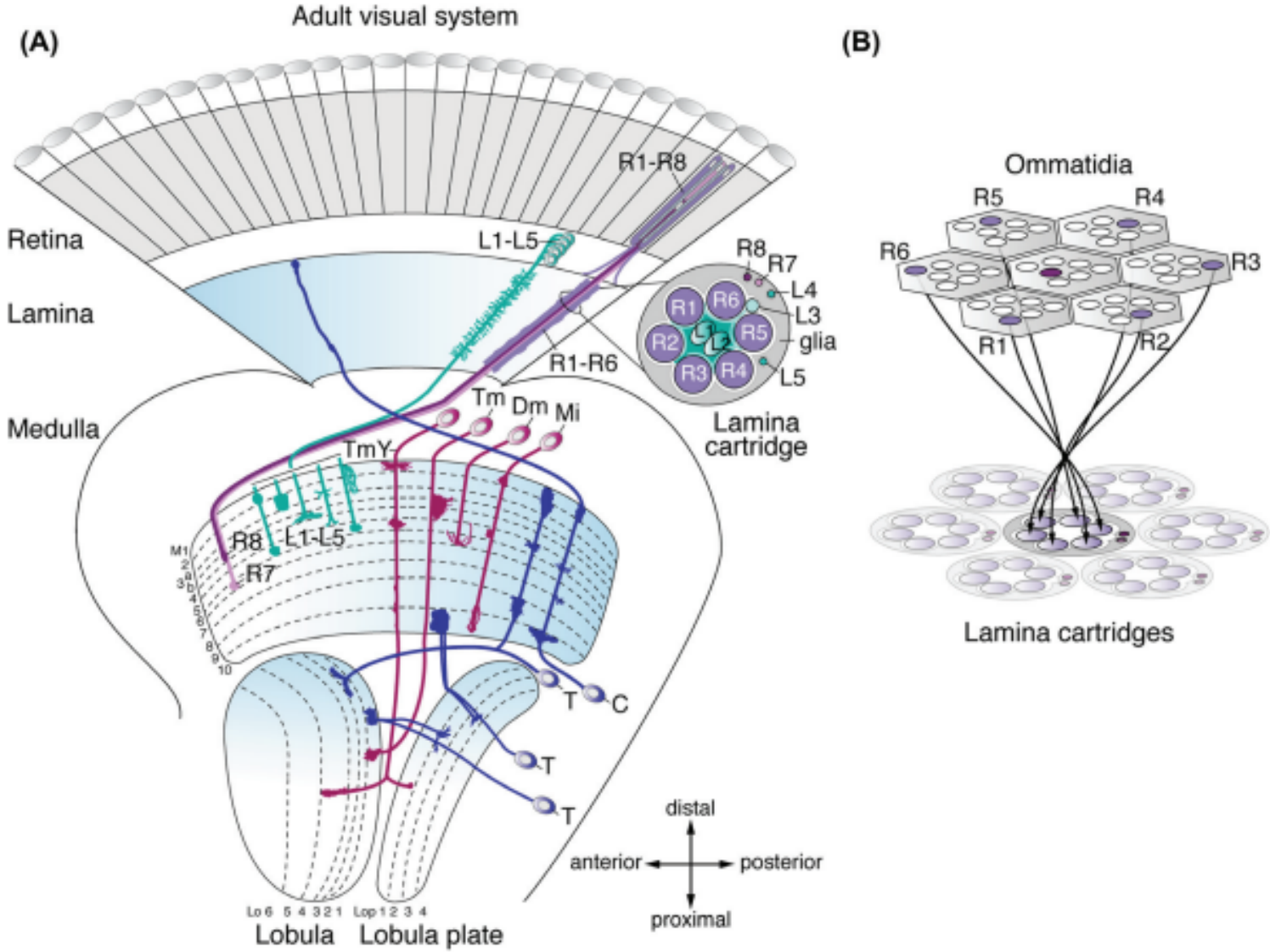

Figure 1. Architecture of the adult *Drosophila* visual system. (**A**) The optic lobe consists of the lamina, medulla, lobula plate, and lobula. The illustration shows a subset of neuron subtypes and their retinotopic projections. R1–R6 cells extend axons from the retina into the lamina, where they connect with lamina neurons L1–L3 in cartridges. Axons of R8 and R7 cells and lamina neurons L1–L5 terminate in one or more of ten medulla neuropil layers (M1–M10). Transmedullary neurons (Tm and TmY) project from the medulla to subsets of six lobula (Lo) and four lobula plate (Lop) neuropil layers. Distal medulla (Dm) neurons innervate several columns in upper medulla layers. Medulla intrinsic (Mi) neurons connect distal and proximal layers. C neurons extend branches into the medulla and lamina. T neurons connect the lobula or lobula plate and medulla, or lobula and lobula plate. (**B**) R1–R6 axons innervate lamina cartridges following the neural superposition principle.

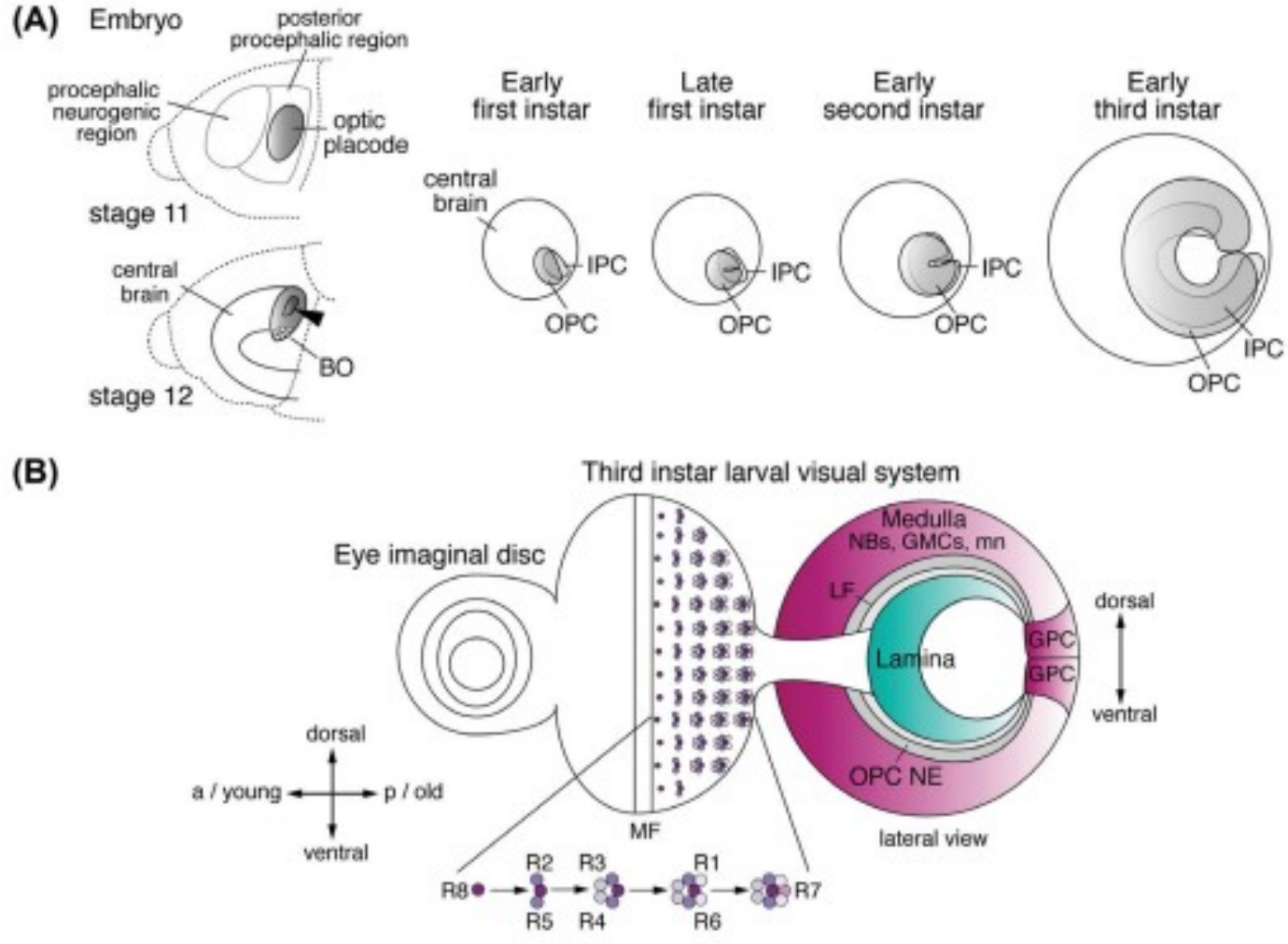

Figure 2. Early optic lobe development and lamina neurogenesis. (**A**) Embryonic stages 11 and 12: the optic placode forms in the posterior procephalic region of the head ectoderm, invaginates (arrowhead), and attaches to the central brain. Ventral cells develop into Bolwig's organ (BO), containing the larval photoreceptor cells. At the early first instar larval stage, the outer and inner proliferation centers (OPC and IPC) are visible. They expand by symmetric divisions and become crescent-shaped during the late first and early second instar larval stages, respectively. The OPC and IPC separate, as they begin to produce offspring from the early third instar larval stage onward. (**B**) In the third instar larval eye imaginal disc, rows of R-cell clusters progressively arise posteriorly (p) of the morphogenetic furrow (MF). R8 cells sequentially recruit R2/R5, R3/R4, R1/R6, and R7 cells into each cluster. A lateral view of the optic lobe shows the crescents of the lamina, the OPC neuroepithelium (NE) and medulla NBs, GMCs, and medulla neurons (mn). Lamina neurogenesis occurs in the wake of the lamina furrow (LF). Glial precursor cell (GPC) areas are located at the dorsal and ventral tips of the OPC crescent. (**C**) A horizontal

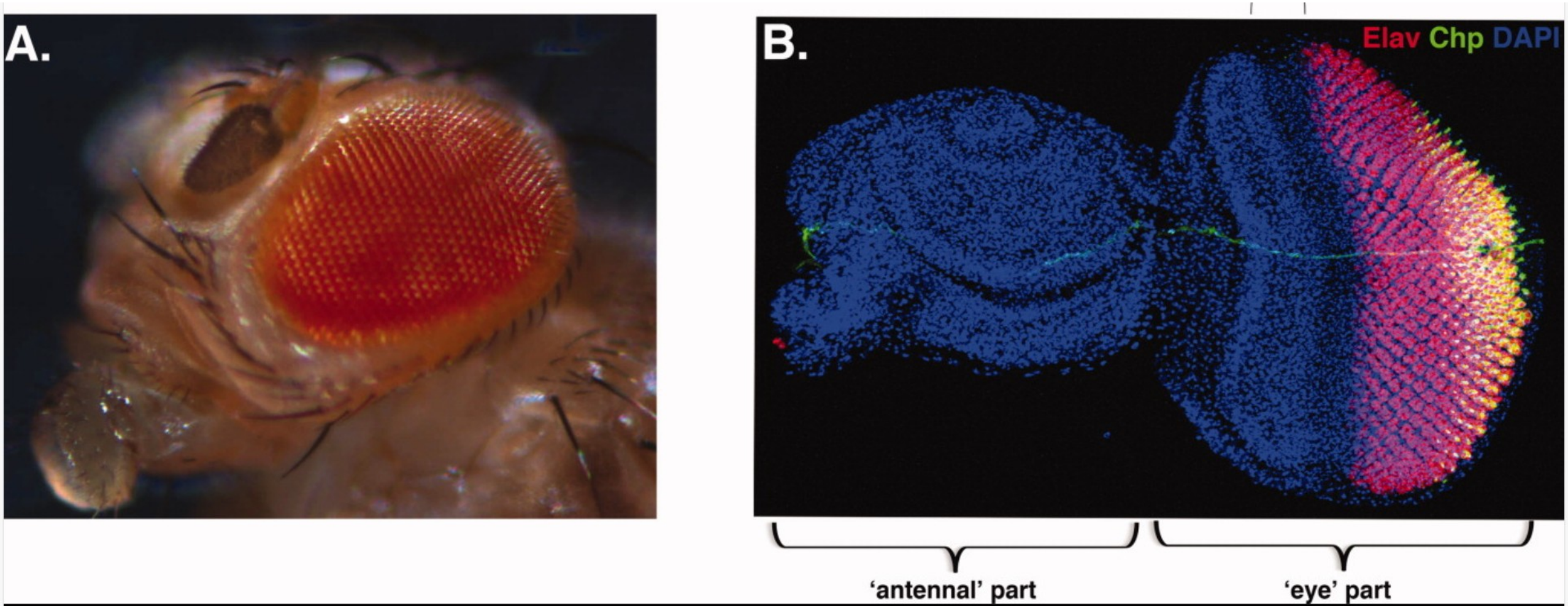
A.
B.
Elav Chp DAPI
'antennal' part
'eye' part

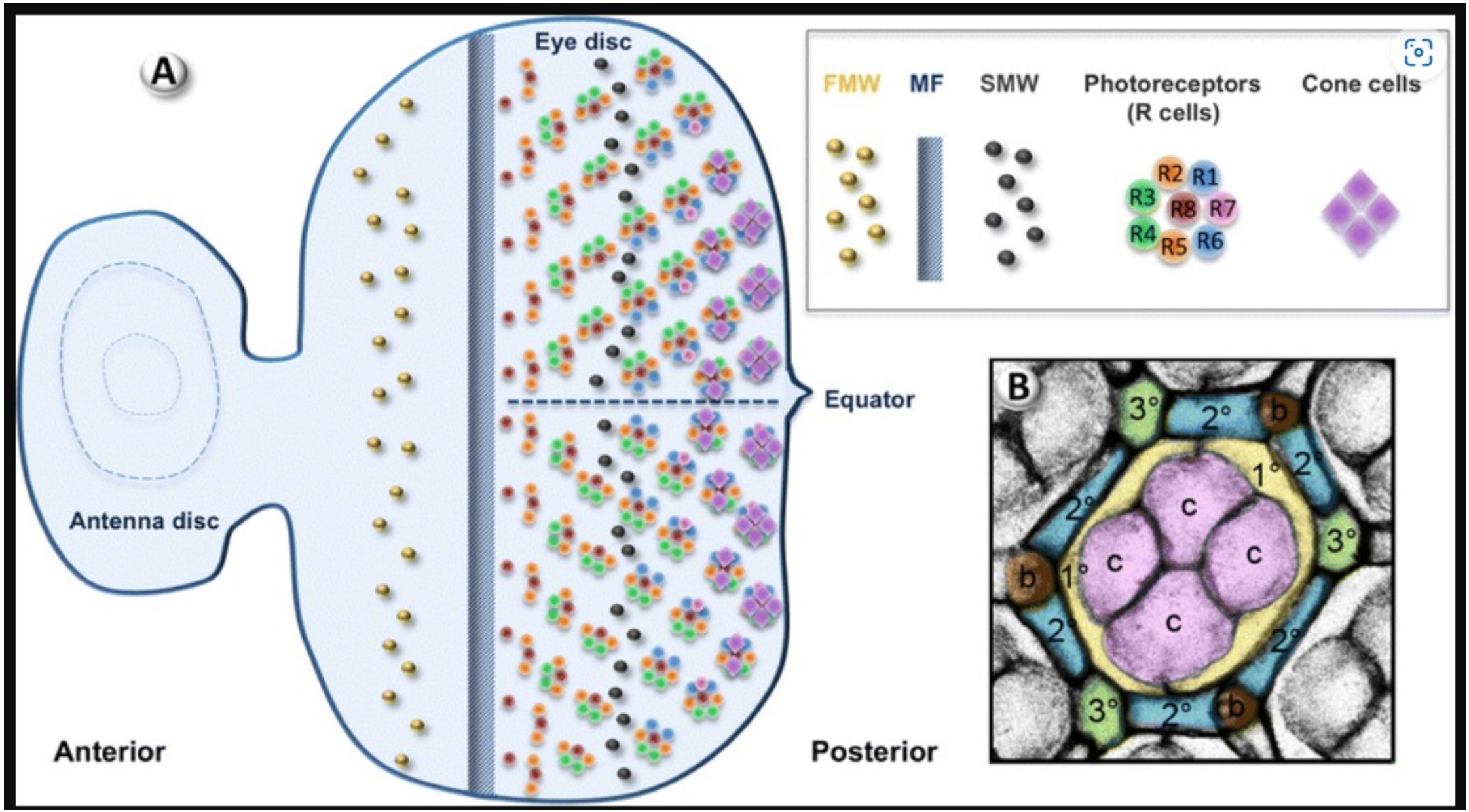
A
Eye disc
Antenna disc
Equator
Anterior
Posterior
FMW
MF
SMW
Photoreceptors
(R cells)
Cone cells
R1
R2
R3
R4
R5
R6
R7
R8
B
1°
2°
3°
b
c

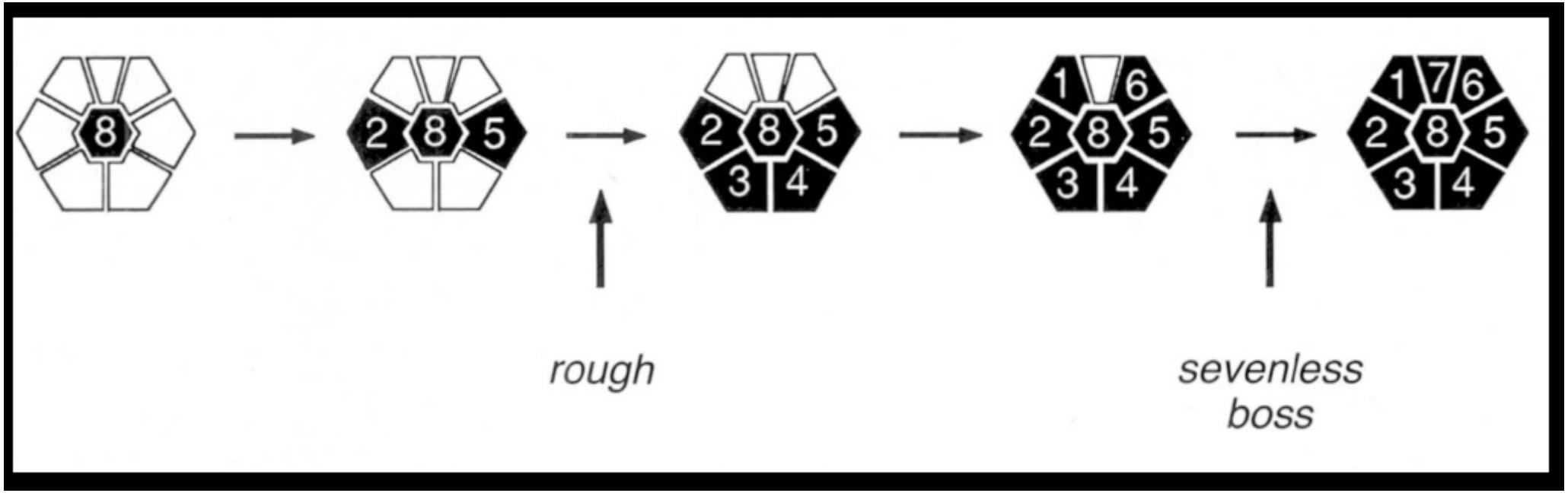
8
2 8 5
2 8 5
3 4
1 6
2 8 5
3 4
1 7 6
2 8 5
3 4
rough
sevenless
boss

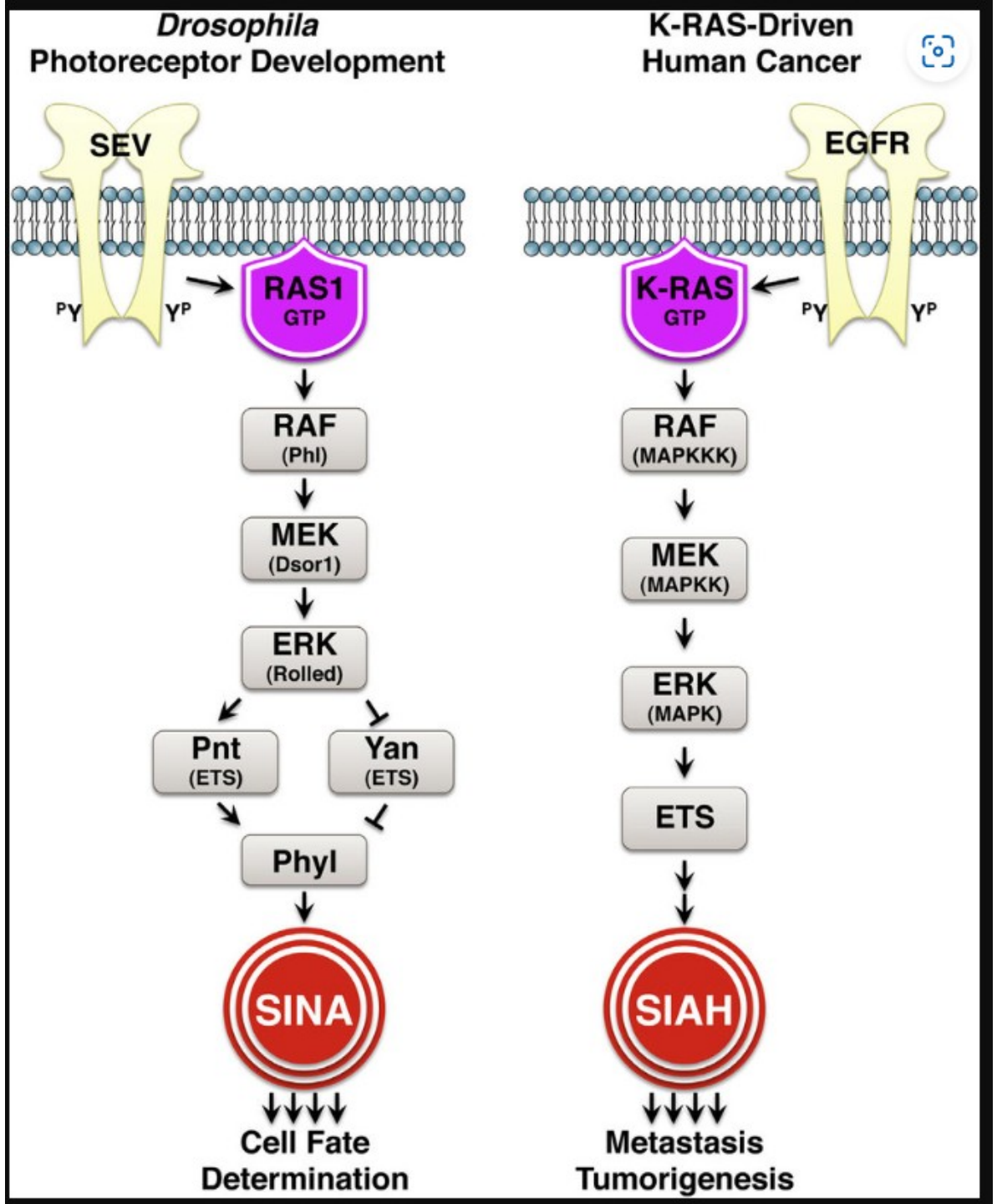
Drosophila
Photoreceptor Development
SEV
PY
YP
RAS1
GTP
RAF
(Phl)
MEK
(Dsor1)
ERK
(Rolled)
Pnt
(ETS)
Yan
(ETS)
Phyl
SINA
Cell Fate
Determination
K-RAS-Driven
Human Cancer
EGFR
PY
YP
K-RAS
GTP
RAF
(MAPKKK)
MEK
(MAPKK)
ERK
(MAPK)
ETS
SIAH
Metastasis
Tumorigenesis

J. Neurogenetics, 28(3–4): 233–249

ISSN: 0167-7063 print/1563-5260 online
DOI: 10.3109/01677063.2014.922558

informa
healthcare

Review

A Challenge of Numbers and Diversity: Neurogenesis in the *Drosophila* Optic Lobe

Holger Apitz and Iris Salecker
Division of Molecular Neurobiology, MRC National Institute for Medical Research, London NW7 1AA, UK

Abstract: The brain areas that endow insects with the ability to see consist of remarkably complex neural circuits. Reiterated arrays of many diverse neuron subtypes are assembled into modular yet coherent functional retinotopic maps. Tremendous progress in developing genetic tools and cellular markers over the past years advanced our understanding of the mechanisms that control the stepwise production and differentiation of neurons in the visual system of *Drosophila melanogaster*. The postembryonic optic lobe utilizes at least two modes of neurogenesis that are distinct from other parts of the fly central nervous system. In the first optic ganglion, the lamina, neuroepithelial cells give rise to precursor cells, whose proliferation and differentiation depend on anterograde signals from photoreceptor axons. In the second optic ganglion, the medulla, the coordinated activity of four signaling pathways orchestrates the gradual conversion of neuroepithelial cells into neuroblasts, while a specific cascade of temporal identity transcription factors controls subtype diversification of their progeny.

Keywords: *Drosophila* visual system, neural stem cells, outer proliferation center, proneural wave, temporal patterning

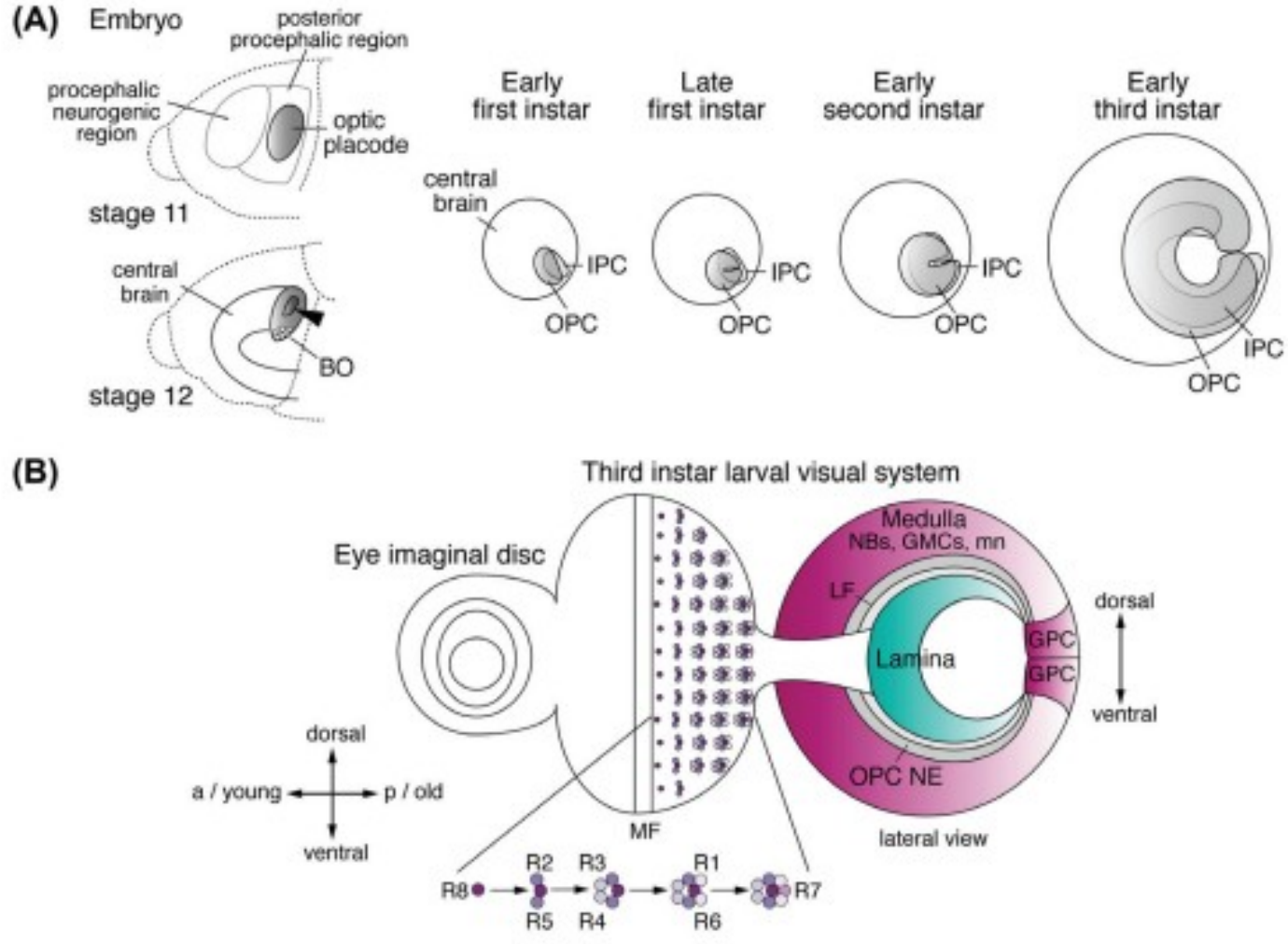

Figure 2. Early optic lobe development and lamina neurogenesis. (**A**) Embryonic stages 11 and 12: the optic placode forms in the posterior procephalic region of the head ectoderm, invaginates (arrowhead), and attaches to the central brain. Ventral cells develop into Bolwig's organ (BO), containing the larval photoreceptor cells. At the early first instar larval stage, the outer and inner proliferation centers (OPC and IPC) are visible. They expand by symmetric divisions and become crescent-shaped during the late first and early second instar larval stages, respectively. The OPC and IPC separate, as they begin to produce offspring from the early third instar larval stage onward. (**B**) In the third instar larval eye imaginal disc, rows of R-cell clusters progressively arise posteriorly (p) of the morphogenetic furrow (MF). R8 cells sequentially recruit R2/R5, R3/R4, R1/R6, and R7 cells into each cluster. A lateral view of the optic lobe shows the crescents of the lamina, the OPC neuroepithelium (NE) and medulla NBs, GMCs, and medulla neurons (mn). Lamina neurogenesis occurs in the wake of the lamina furrow (LF). Glial precursor cell (GPC) areas are located at the dorsal and ventral tips of the OPC crescent. (**C**) A horizontal

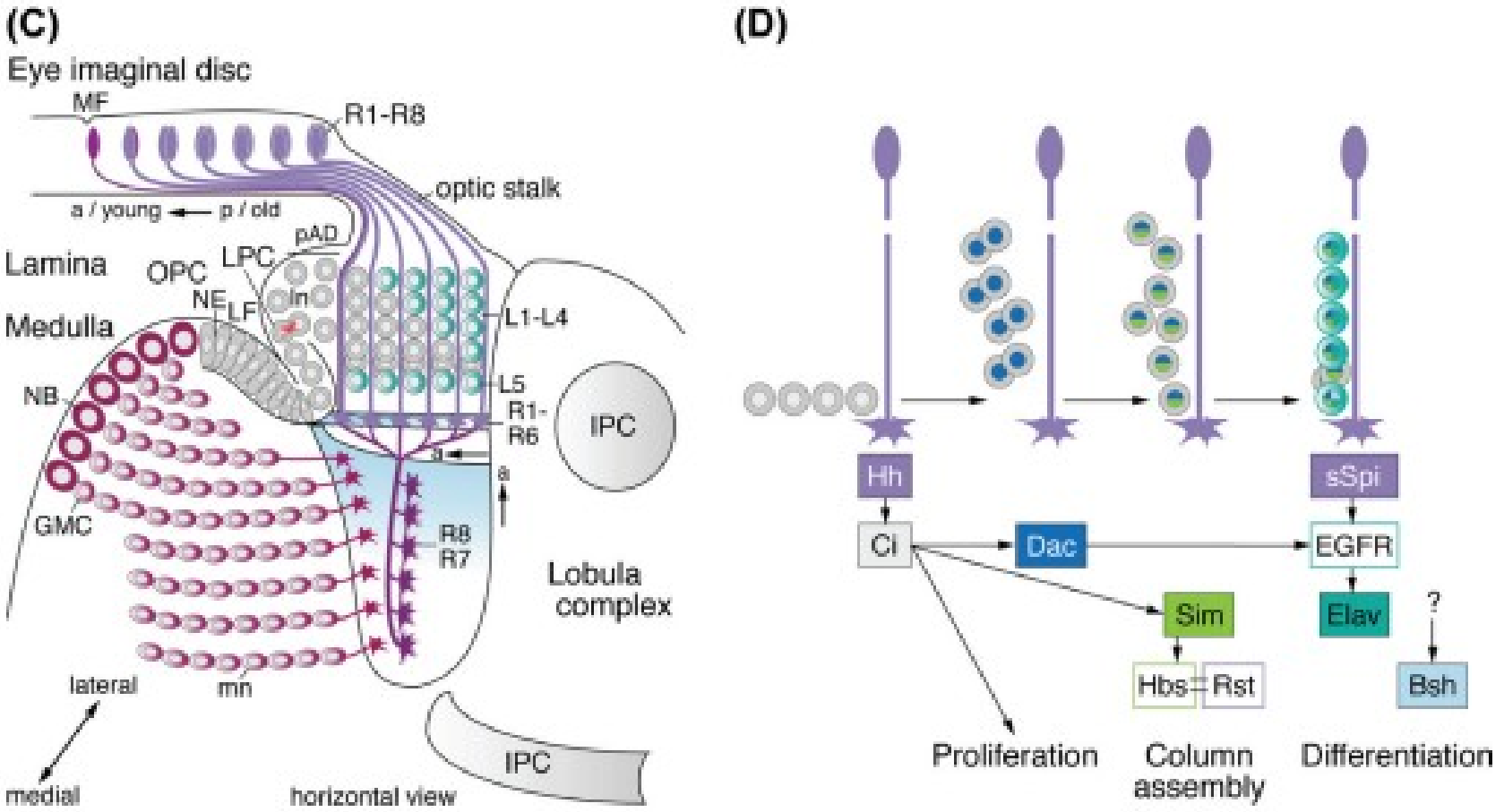

the lamina furrow (LF). Glial precursor cell (GPC) areas are located at the dorsal and ventral tips of the OPC crescent. (**C**) A horizontal view of the third instar larval eye imaginal disc and optic lobe shows the stepwise formation of lamina neurons (ln) and medulla neurons. Medially, the OPC NE gives rise to medulla NBs, GMCs and medulla neurons. Laterally, the OPC NE generates lamina precursor cells (LPCs). The position of the NE to LPC conversion at the bottom of the lamina furrow is approximate in this schematic presentation. LPCs give rise to undifferentiated lamina neurons in the pre-assembly domain (pAD). Lamina neurons assemble into columns in close association with R-cell bundles and differentiate into neuronal subtypes L1–L5. The IPC produces neurons of the lobula complex. (**D**) R-cell axons provide the anterograde signals Hedgehog (Hh) and Spitz (sSpi) to control LPC proliferation, lamina column assembly and lamina neuron differentiation. a, anterior; Bsh, Brain-specific homeobox; Ci, Cubitus interruptus; Dac, Dachshund; EGFR, epidermal growth factor receptor; Elav, Embryonic lethal abnormal vision; Hbs, Hibris; Sim, Single-minded; Rst, Roughest.

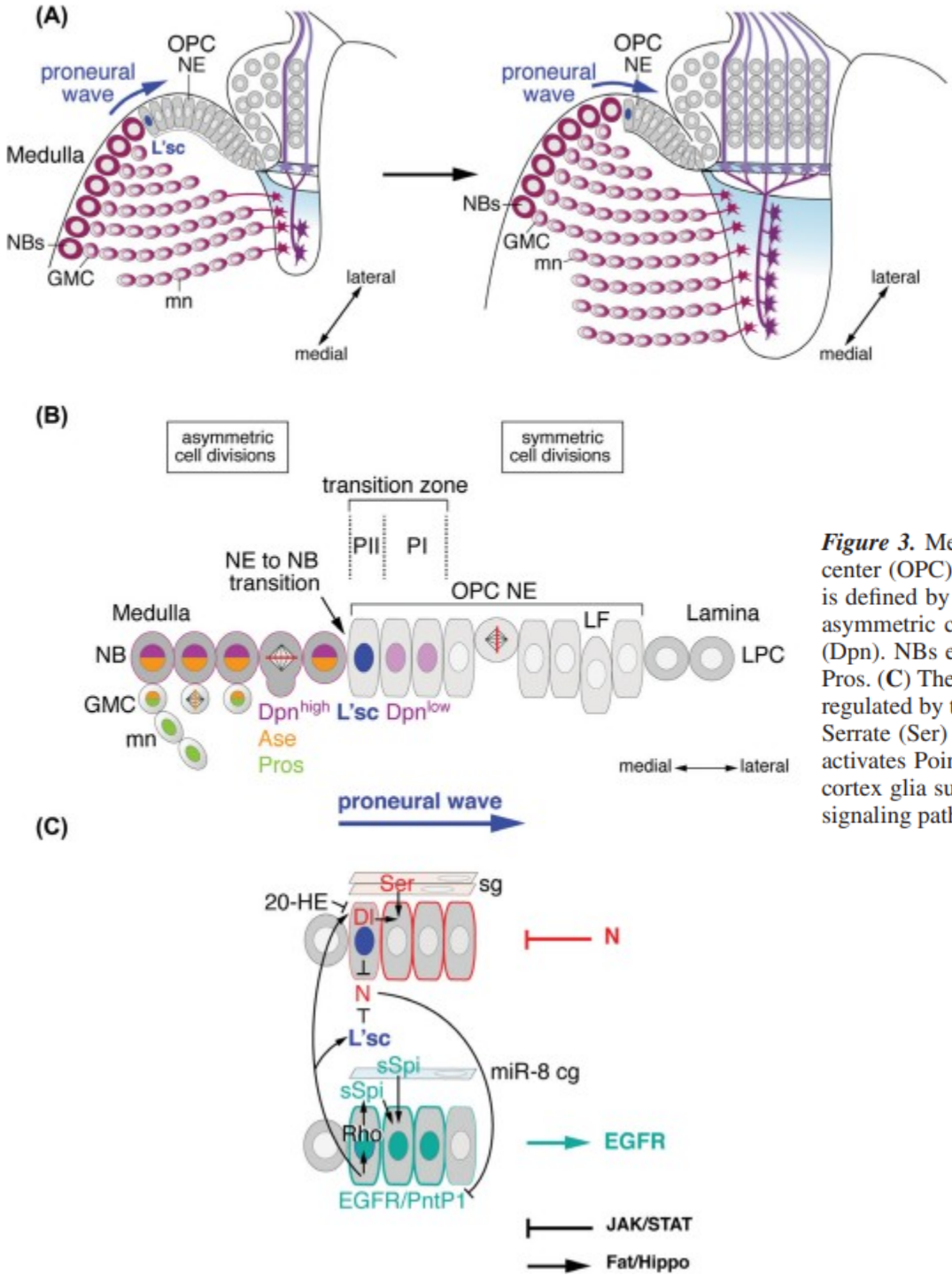

Figure 3. Medulla neurogenesis depends on the sequential conversion of neuroepithelial (NE) cells to NBs. (**A**) Outer proliferation center (OPC) NE cells gradually convert into medulla NBs in a medial to lateral orientation. The advancement of the proneural wave is defined by Lethal of scute (L'sc) expression. (**B**) The gradual conversion of NE cells to NBs involves a switch from symmetric to asymmetric cell divisions. The transition zone consists of progenitors PII expressing L'sc and PI expressing low levels of Deadpan (Dpn). NBs express Dpn and Asense (Ase). GMCs express Ase and Prospero (Pros). Newly formed medulla neurons (mn) maintain Pros. (**C**) The progression of the proneural wave from medial to lateral is negatively regulated by the Notch (N) pathway and positively regulated by the epidermal growth factor receptor (EGFR) pathway. N signaling is activated in PI NE cells by Delta (Dl) in PII and by Serrate (Ser) in surface glia (sg). Dl expression is repressed by Ecdysone (20-HE, 20-Hydroxyecdysone) signaling. EGFR signaling activates Pointed P1 (PntP1) and Rhomboid (Rho), which promote the secretion of Spitz (sSpi) from PII. sSpi is also provided by a cortex glia subtype (cg) expressing the microRNA *miR-8*. N and EGFR signaling regulate each other. The JAK/STAT and Fat/Hippo signaling pathways provide additional negative and positive inputs, respectively. LF, lamina furrow; LPC, lamina precursor cells.

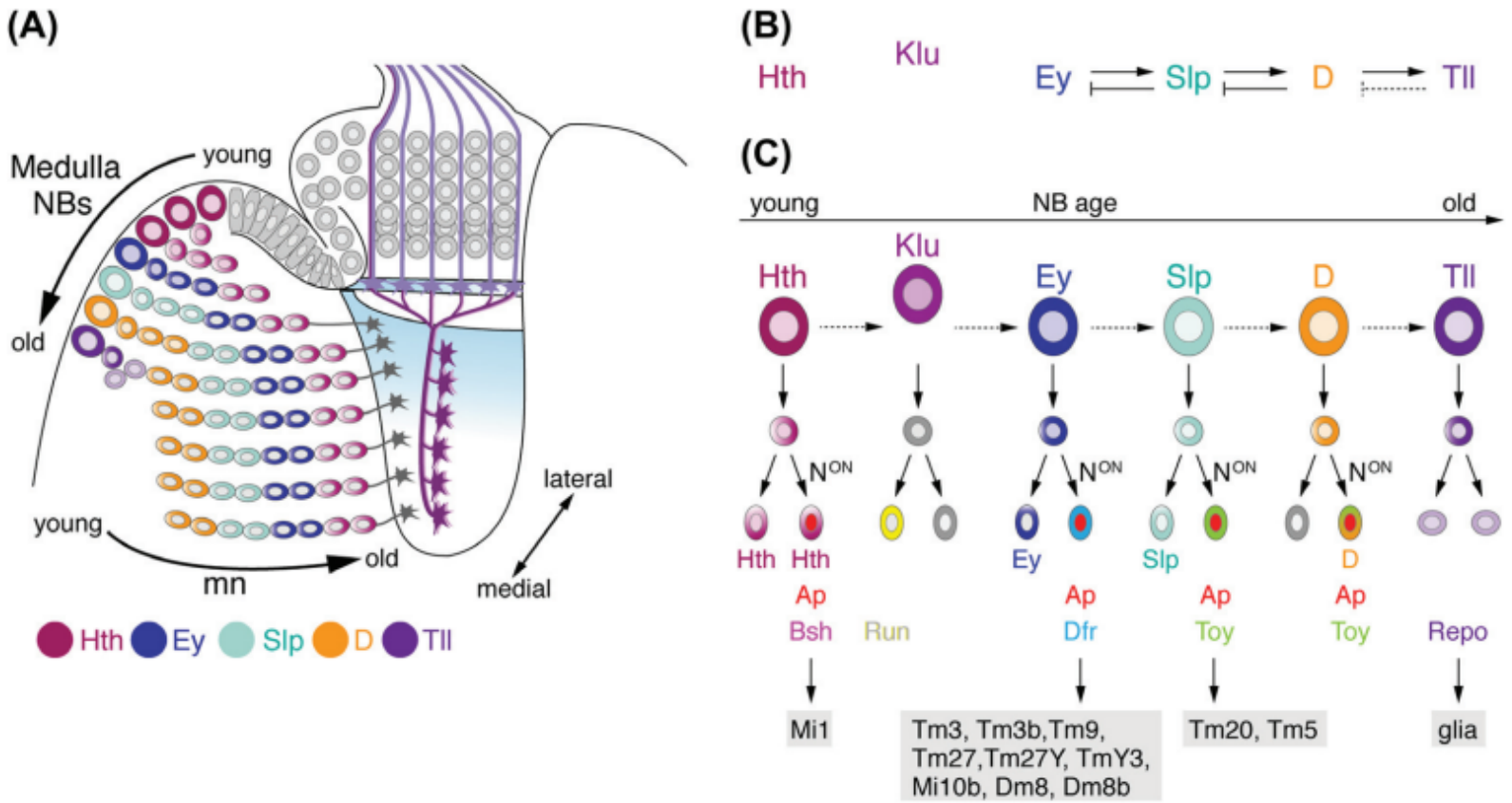

Figure 4. Temporal patterning of medulla NBs and Notch (N) signaling contribute to the generation of diverse neuron subtypes. (**A**) NE cells gradually convert into NBs. As medulla NBs age, they sequentially express the transcription factors Homothorax (Hth), Eyeless (Ey), Sloppy paired 1 and 2 (Slp), Dichaete (D), and Tailless (Tll). Each NB produces a column of medulla neurons. Progeny maintain the expression of the determinant present in the NB at the time of their birth. Older NBs and their offspring are located more medially. In each lineage, the oldest neurons are positioned closest to the medulla neuropil. Klumpfuss (Klu) is expressed in NBs but not in progeny and therefore has not been included in this schematic. Interim stages, during which NBs express more than one factor and neurons downregulating factors are also not shown. (**B**) Ey, Slp, and D are required for the transition to the next determinant. Slp, D, and Tll are necessary to repress the preceding factor in the series. Tll is sufficient but not required to repress D (dashed line). (**C**) N-mediated binary cell fate choices further diversify lineages. Progeny, in which N signaling is on, express Apterous (Ap). Depending on the combination of transcription factors present, the expression of subtype-identity determinants such as Brain-specific homeobox (Bsh), Runt (Run), Drifter (Dfr), or Twin of Eyeless (Toy) is induced. Lineages defined by the combinatorial expression of these determinants give rise to specific neuronal subtypes. Tll-positive NBs generate Reversed polarity (Repo)-positive glia. Dm, distal medulla neurons; Mi, medulla intrinsic neurons; Tm, transmedullary neurons; TmY, transmedullary Y neurons.

OXFORD GENETICS

GENETICS, 2023, 224(2), iyad064
https://doi.org/10.1093/genetics/iyad064
Advance Access Publication Date: 2 May 2023
FlyBook

Visual processing in the fly, from photoreceptors to behavior

Timothy A. Currier,† Michelle M. Pang,† Thomas R. Clandinin*

Department of Neurobiology, Stanford University School of Medicine, Stanford, CA 94305, USA

*Corresponding author: Department of Neurobiology, Stanford University School of Medicine, 299 W. Campus Drive, Stanford, CA 94305, USA. Email: trc@stanford.edu
†These authors contributed equally.

Abstract

Originally a genetic model organism, the experimental use of *Drosophila melanogaster* has grown to include quantitative behavioral analyses, sophisticated perturbations of neuronal function, and detailed sensory physiology. A highlight of these developments can be seen in the context of vision, where pioneering studies have uncovered fundamental and generalizable principles of sensory processing. Here we begin with an overview of vision-guided behaviors and common methods for probing visual circuits. We then outline the anatomy and physiology of brain regions involved in visual processing, beginning at the sensory periphery and ending with descending motor control. Areas of focus include contrast and motion detection in the optic lobe, circuits for visual feature selectivity, computations in support of spatial navigation, and contextual associative learning. Finally, we look to the future of fly visual neuroscience and discuss promising topics for further study.

Keywords: neuroscience, vision, anatomy, physiology, computation, behavior, navigation, learning, FlyBook

Tethered flies walking or flying

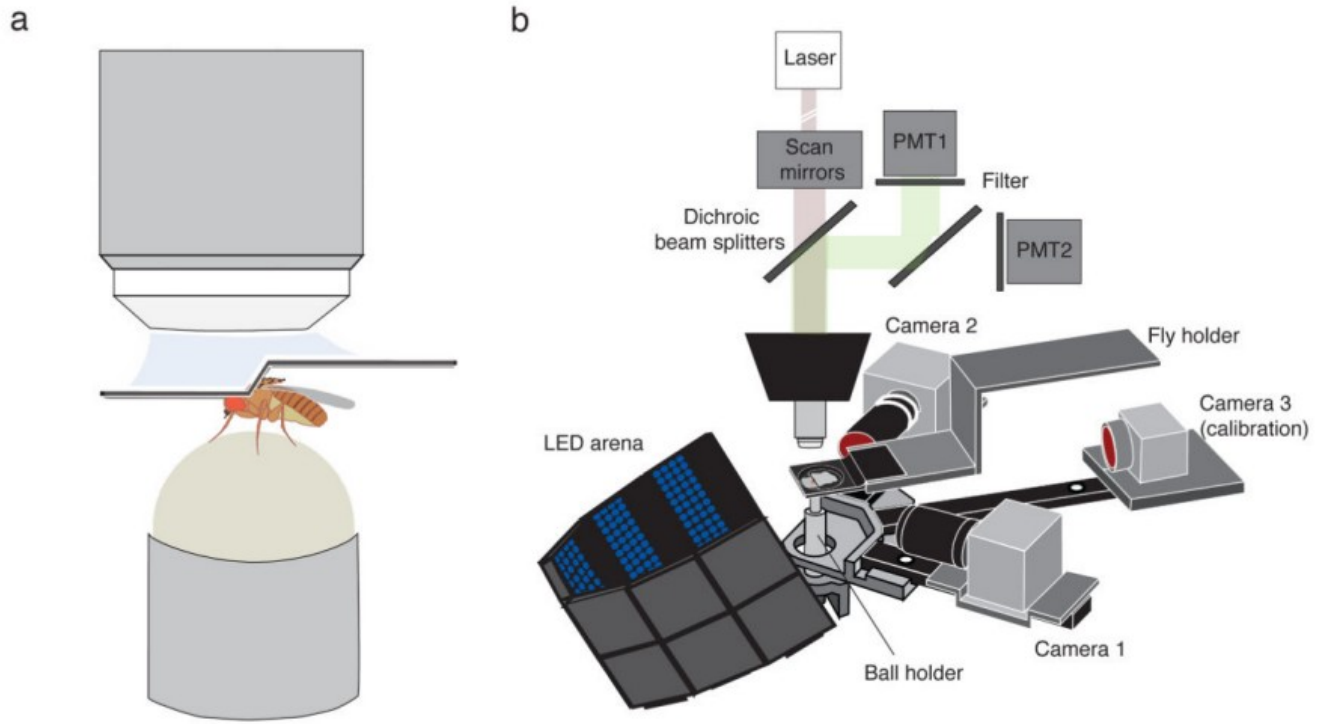

Figure 1. Setup for two-photon imaging from the brain of head-fixed flies walking on a ball
(**a**) Fly holder for tethered walking fly recording separates exposed brain from intact legs and eyes allowing visual stimulation and walking on the ball. (**b**) Schematic showing arrangement of holder, ball, ball trackers, calibration camera, microscope (including a schematic for 2-photon excitation and detection systems), objective and visual arena.

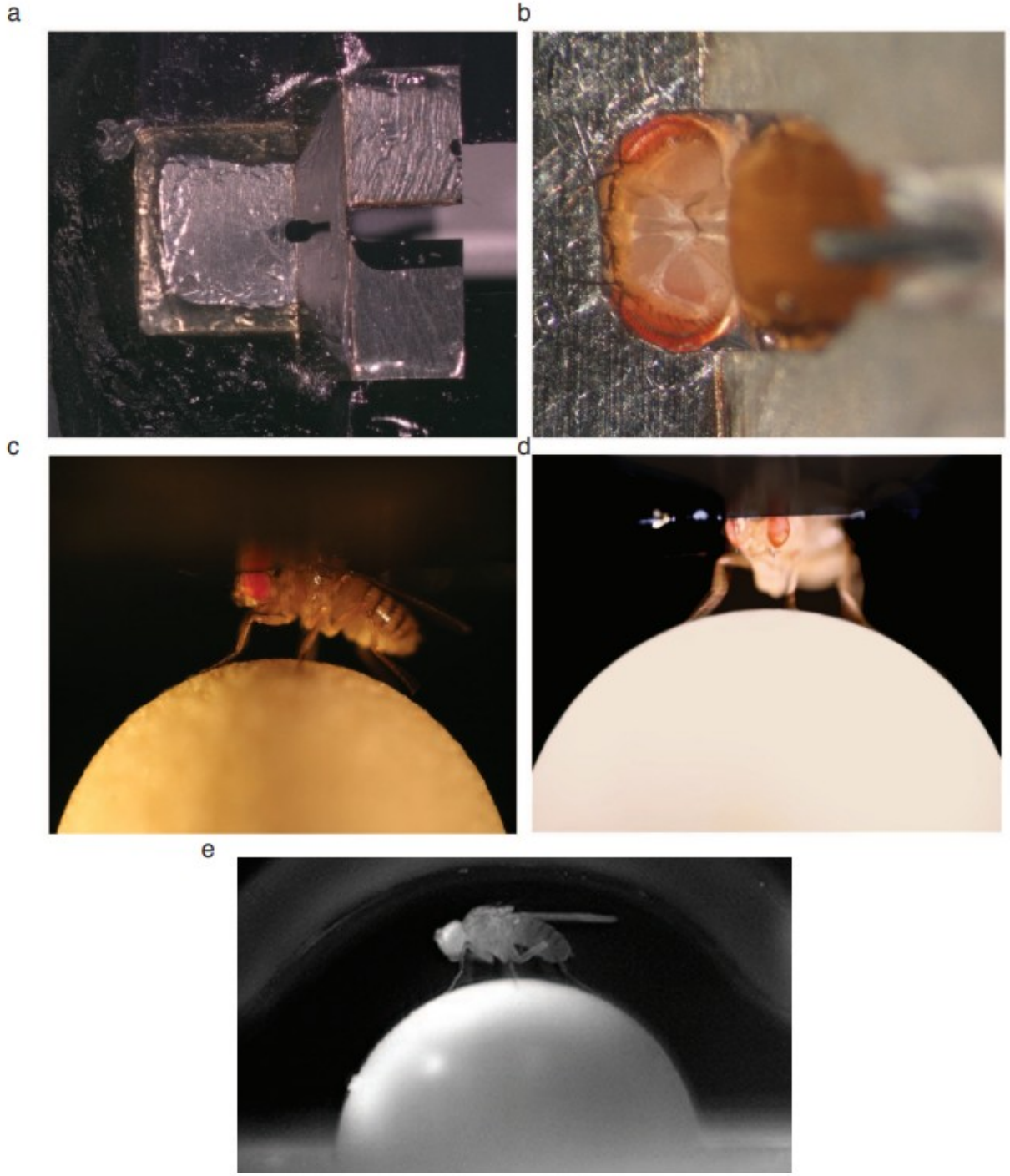

a. Top view of the fly holder. b. Top vi
during mounting is also visible at righ
holder and standing on the ball unde
diameter curved surface.

Neuron 52, 425–436, November 9, 2006 ©2006 Elsevier Inc. DOI 10.1016/j.neuron.2006.08.028

Refined Spatial Manipulation of Neuronal Function by Combinatorial Restriction of Transgene Expression

Neurotechnique

Haojiang Luan,[1] Nathan C. Peabody,[1]
Charles R. Vinson,[2] and Benjamin H. White[1,*]
[1] Laboratory of Molecular Biology
National Institute of Mental Health
[2] Laboratory of Metabolism
National Cancer Institute
National Institutes of Health
9000 Rockville Pike
Bethesda, Maryland 20892

Summary

Selective genetic manipulation of neuronal function in vivo requires techniques for targeting gene expression to specific cells. Existing systems accomplish this using the promoters of endogenous genes to drive expression of transgenes directly in cells of interest or, in "binary" systems, to drive expression of a transcription factor or recombinase that subsequently activates the expression of other transgenes. All such techniques are constrained by the limited specificity of the available promoters. We introduce here a combinatorial system in which the DNA-binding (DBD) and transcription-activation (AD) domains of a transcription factor are independently targeted using two different promoters. The domains heterodimerize to become transcriptionally competent and thus drive transgene expression only at the intersection of the expression patterns of the two promoters. We use this system to dissect a neuronal network in *Drosophila* by selectively targeting expression of the cell death gene *reaper* to subsets of neurons within the network.

component. In *Drosophila*, the Gal4-UAS system (reviewed in Duffy, 2002), which uses the yeast transcription factor Gal4 to activate expression of transgenes placed downstream of its unique "upstream activating sequence," or UAS, has been augmented by the addition of the Gal4 repressor, Gal80. Targeting of Gal80 expression to subsets of cells can then be used to restrict gene expression (Suster et al., 2004), in some cases with single-cell resolution, as in the widely used MARCM system (Lee and Luo, 1999). Alternatively, a "Flp-in" technique, which makes UAS-transgene activation contingent on excision of an inserted "stop cassette" by the Flp-recombinase, has been used to restrict expression by independently targeting Gal4 and Flp using different promoters (Stockinger et al., 2005). Similarly in mice, transgene activation has been made contingent on the activity of two independently targeted recombinases by coupling Flp to the Cre-lox system, as in the "intersectional gene activation" technique (Awatramani et al., 2003; Farago et al., 2006).

To date, ternary systems have been developed primarily for use in developmental studies to restrict reporter transgene expression to small numbers of neurons for lineage analysis and fate mapping. Most can, in principle, also be used to drive effector transgene expression to manipulate neuronal function, but usually with certain limitations. Restriction using the MARCM technique, for example, is limited to clonally derived neurons and constrained by the developmental timing of mitosis in the lineages under study. In recombinase-based systems, inefficiency of recombination can limit the extent of gene activation (Ting et al., 2005). Such systems are also intrinsically irreversible.

To develop an alternative ternary approach for versa-

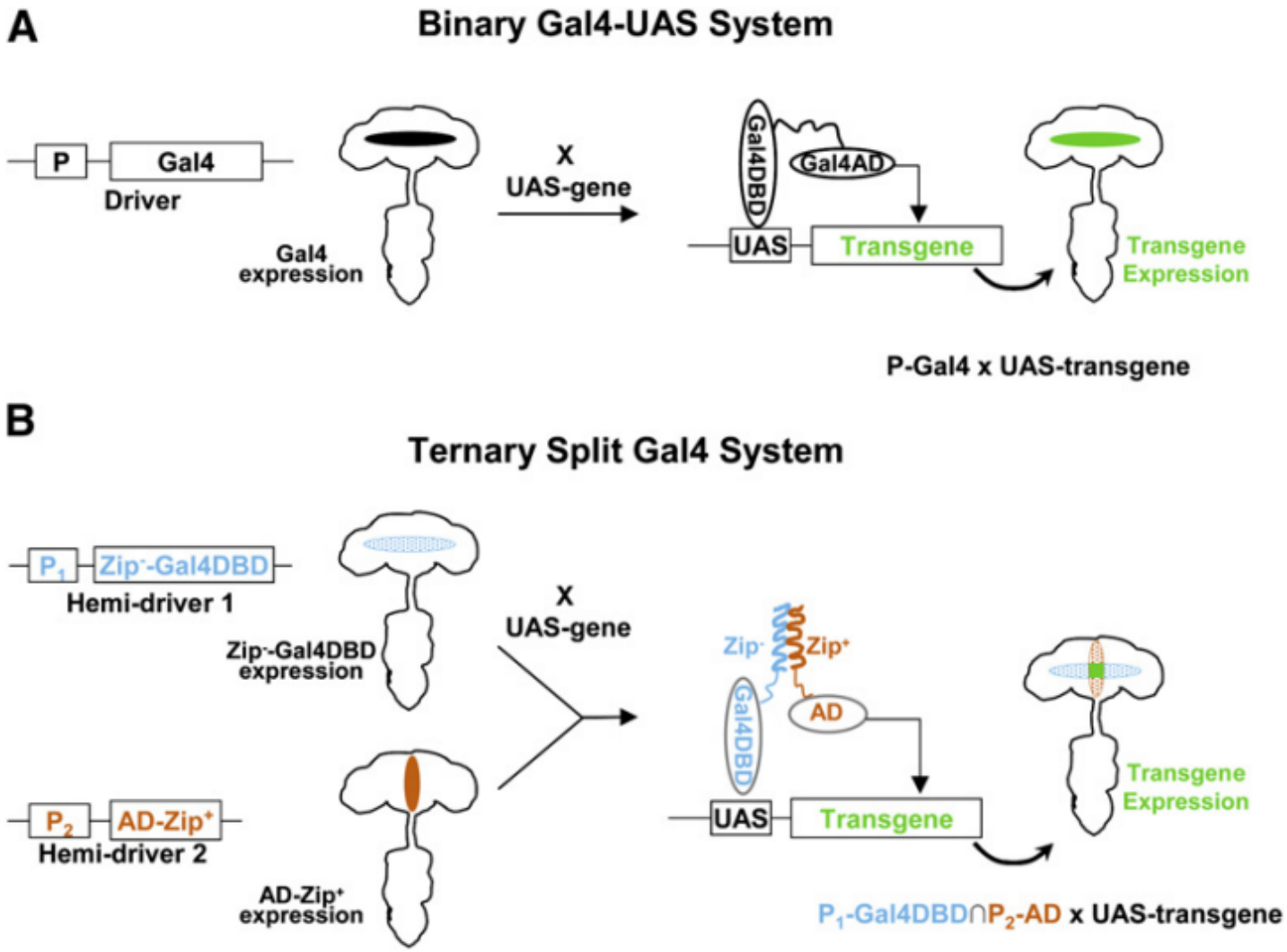

Figure 1. The Ternary Split Gal4 System Improves upon Existing Binary Expression Systems in Restricting Transgene Expression

(A) Schematic depiction of the Gal4-UAS system of *Drosophila,* a classic binary system for targeting transgene expression in vivo. The first essential component of this system, shown at left, is a transgene containing the yeast transcription factor Gal4 downstream of a promoter/enhancer (P). P drives expression of Gal4 in flies bearing this transgene in a cell type-specific manner (shown as a black region within the CNS). When flies bearing Gal4 are crossed to flies bearing the second component of the system, a transgene of interest placed downstream of the Gal4 DNA recognition site or UAS, this transgene is also expressed in the same cell type-specific manner (right).

(B) The Split Gal4 system exploits the fact that the two functional domains of Gal4, the DNA-binding (DBD) and transcription-activation (AD) domains, are separable. In the Split Gal4 system each domain is fused to a heterodimerizing leucine zipper (Zip^+ or Zip^-) to insure that the two domains associate when expressed in the same cell and reconstitute transcriptional activity. Starting at left, the schematic shows that the Gal4DBD and AD constructs can be independently targeted using different promoters/enhancers (P_1 and P_2). When these constructs ("hemidrivers") are brought together in crosses to flies bearing a UAS-transgene, the transgene is expressed in progeny only at the intersection of the expression patterns of P_1 and P_2 (designated by the intersection sign, ∩), where transcriptional activity is reconstituted, as shown on the bottom right. The Gal4DBD must be used if UAS-transgenes are to be transcribed, but any transcription-activation domain can be used, as long as it is fused to the leucine zipper fragment complementary to that fused to Gal4DBD.

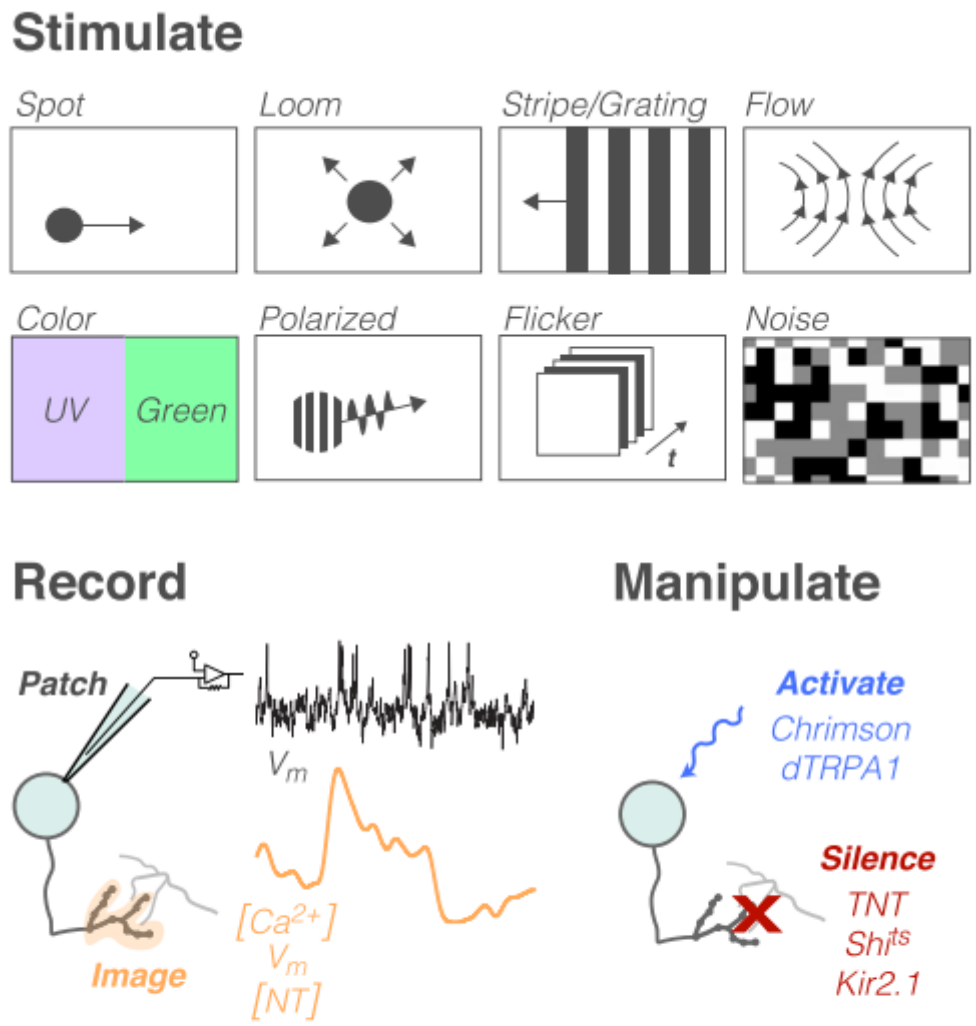

Fig. 1. Tools and techniques to probe visual circuits. Top: illustrations of select visual stimuli. Bottom-left: recording methods. Membrane potential (V_m) can be recorded via both patch clamp and imaging, while intracellular calcium concentration ($[Ca^{2+}]$) and extracellular neurotransmitter concentration ([NT]) are most often measured with optical techniques. Bottom-right: common techniques for manipulating neuron function. See text for additional information about each tool.

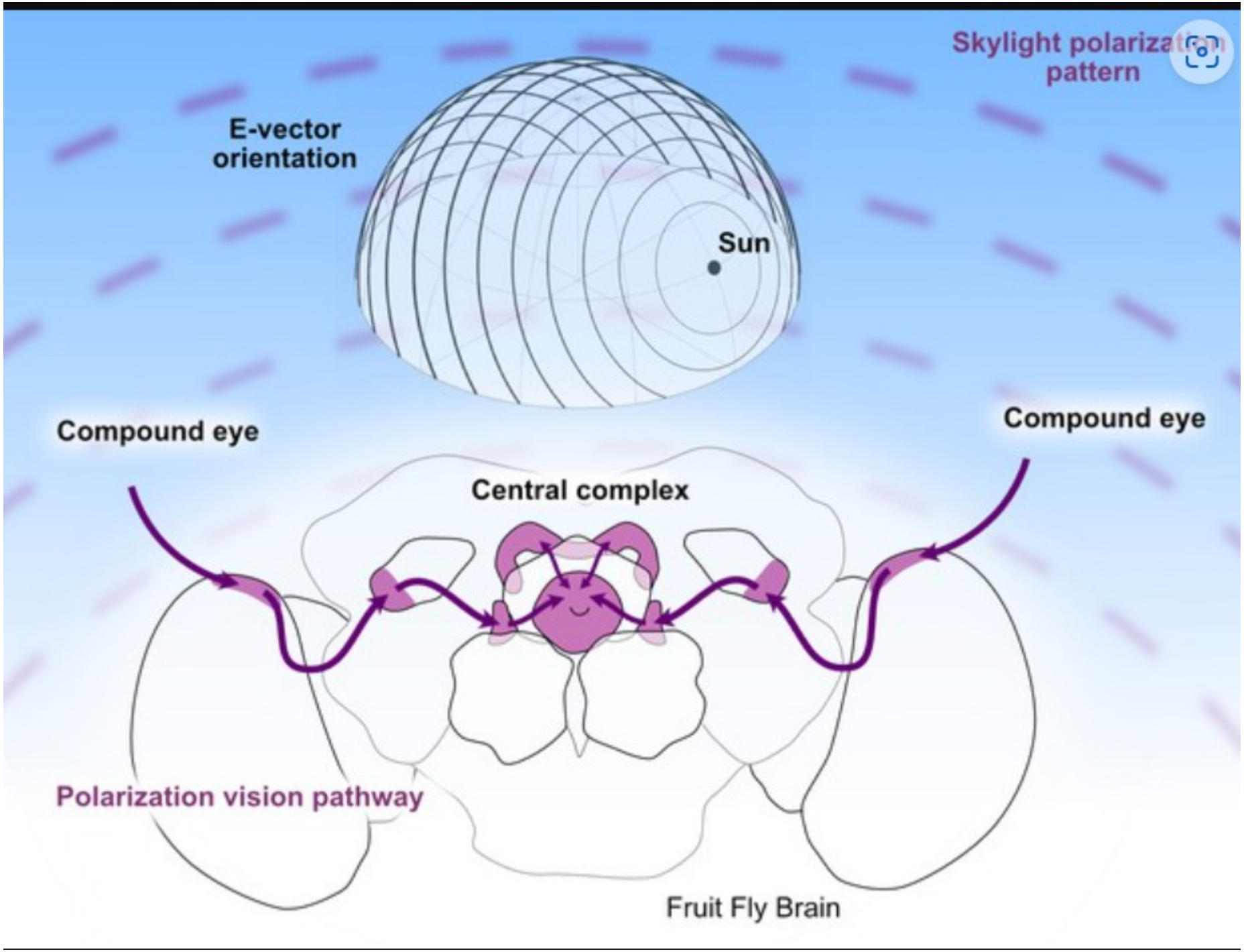
Skylight polarization pattern
E-vector orientation
Sun
Compound eye
Compound eye
Central complex
Polarization vision pathway
Fruit Fly Brain

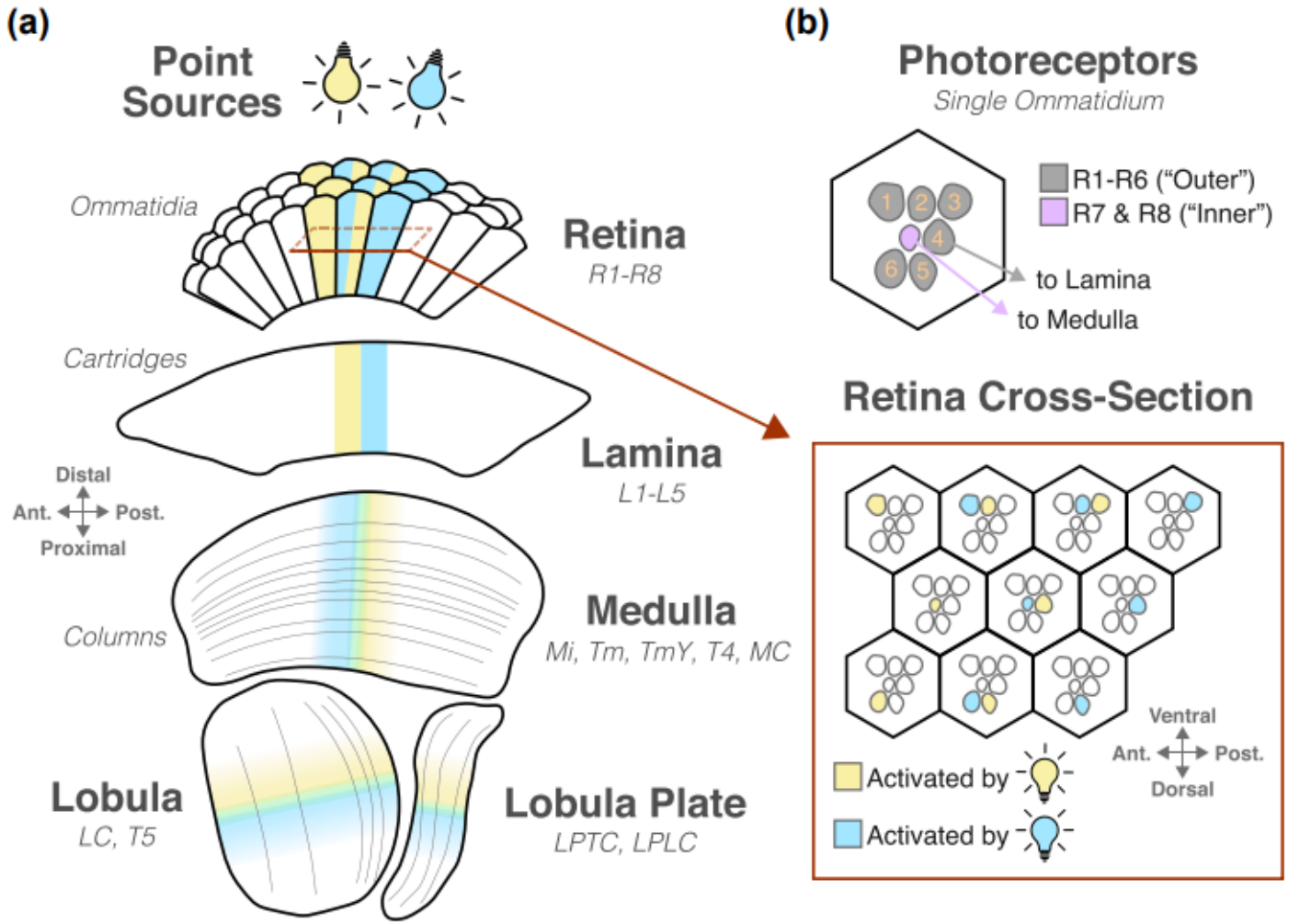

Fig. 2. a) Overview of the compound eye and visual system anatomy. A simplified horizontal section through the optic lobe shows the organization of the early visual system. The portions of each neuropil that are activated by 2 adjacent point sources of light are highlighted in blue and yellow. Green indicates a mixing of signals from both sources. Red box indicates the location of the retinal cross-section shown in b). For regions with prominent laminar organization, layers are shown as thin gray lines. The primary feedforward cell types are listed for each neuropil. b) Top: a simplified cross-section through a single ommatidium shows the spatial arrangement of individual photoreceptors. Bottom: "Superposition" is illustrated in a cross-section through the retina, as indicated by the red box in a). The pattern of photoreceptors that respond to the blue and yellow point sources is shown.

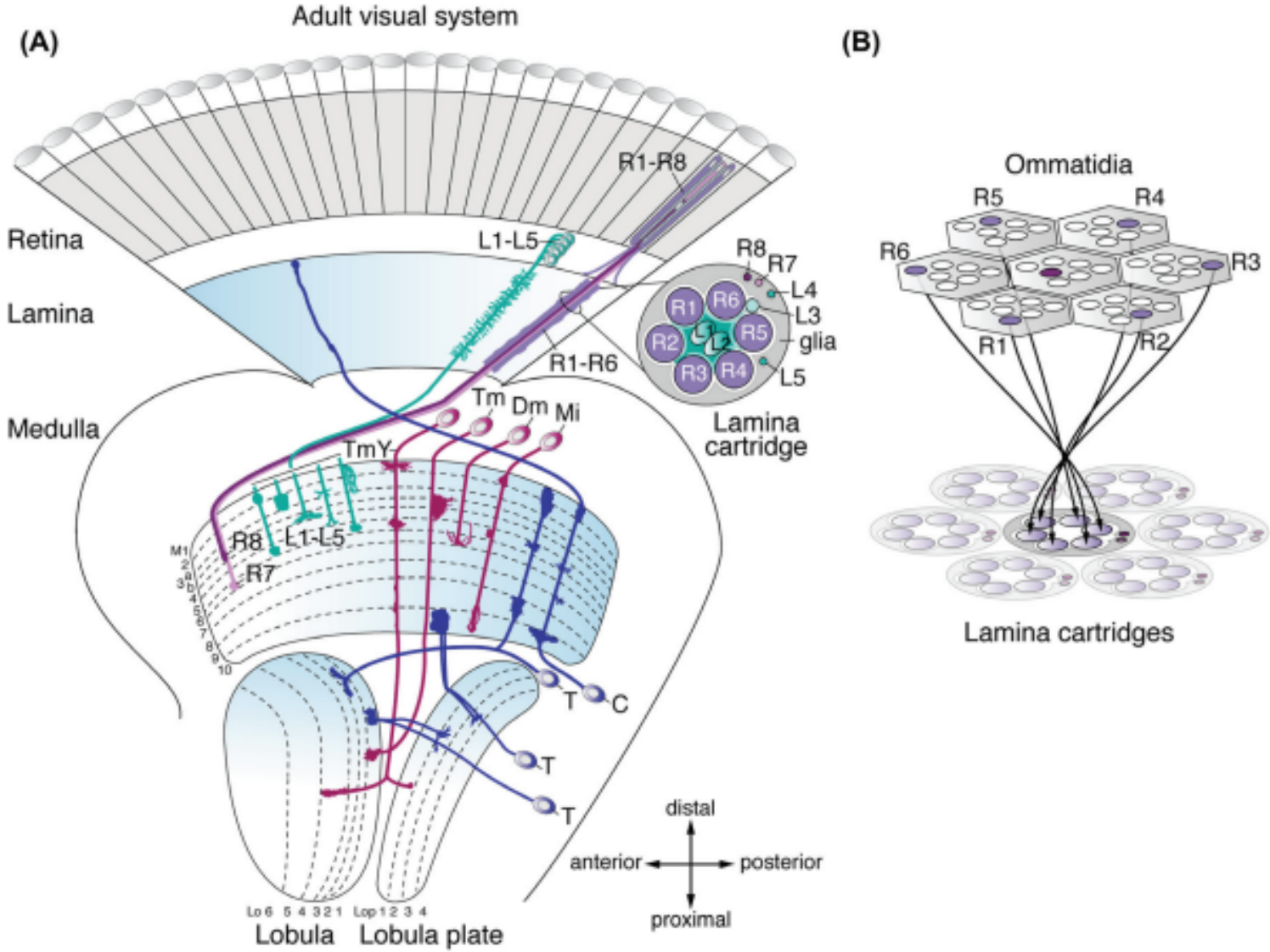

Figure 1. Architecture of the adult *Drosophila* visual system. (**A**) The optic lobe consists of the lamina, medulla, lobula plate, and lobula. The illustration shows a subset of neuron subtypes and their retinotopic projections. R1–R6 cells extend axons from the retina into the lamina, where they connect with lamina neurons L1–L3 in cartridges. Axons of R8 and R7 cells and lamina neurons L1–L5 terminate in one or more of ten medulla neuropil layers (M1–M10). Transmedullary neurons (Tm and TmY) project from the medulla to subsets of six lobula (Lo) and four lobula plate (Lop) neuropil layers. Distal medulla (Dm) neurons innervate several columns in upper medulla layers. Medulla intrinsic (Mi) neurons connect distal and proximal layers. C neurons extend branches into the medulla and lamina. T neurons connect the lobula or lobula plate and medulla, or lobula and lobula plate. (**B**) R1–R6 axons innervate lamina cartridges following the neural superposition principle.

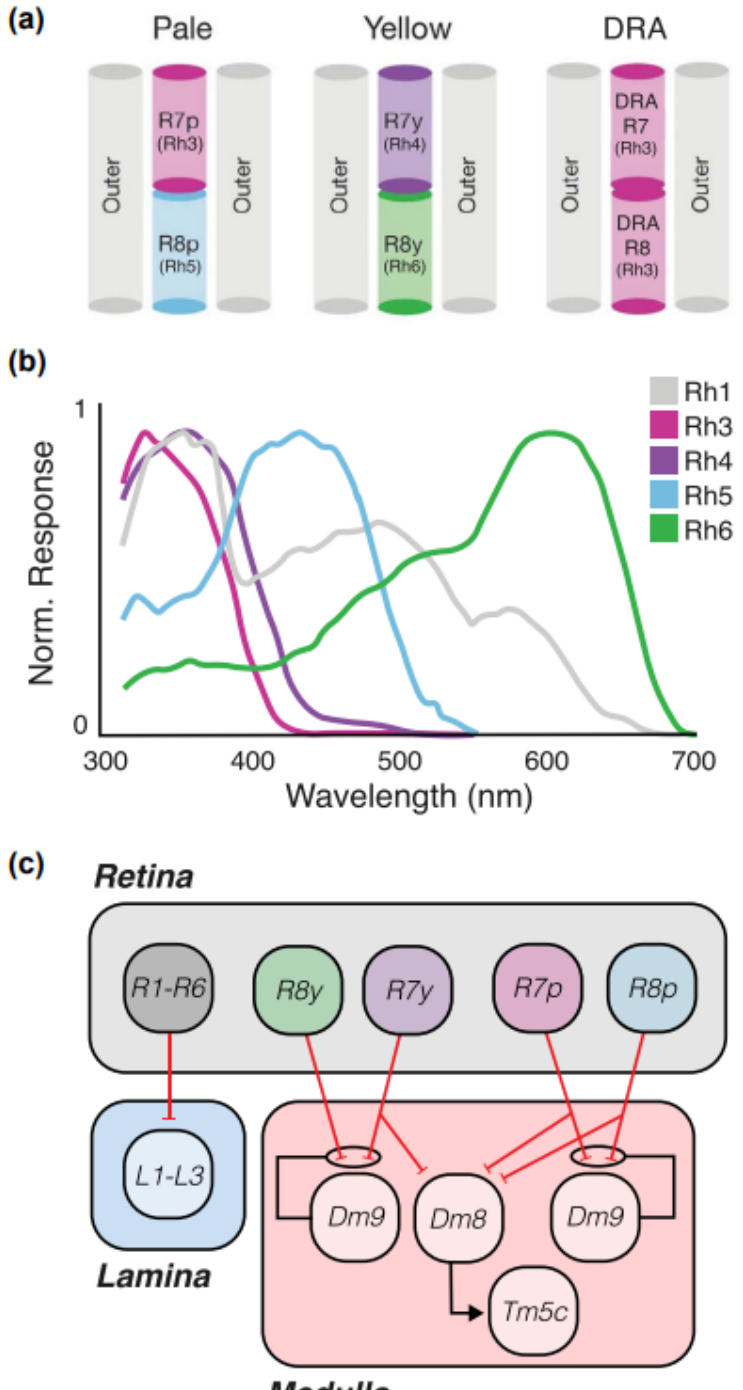

Fig. 3. Photoreceptors transduce light of specific wavelength. a) Arrangement of photoreceptors in pale, yellow, and dorsal rim area ommatidia. In all cases, R1–R6 outer photoreceptors flank stacked R7 and R8 inner photoreceptors. The rhodopsin variants expressed in R7 and R8 determine ommatidium type. Adapted from Sharkey *et al.* (2020). b) Normalized photoreceptor responses by wavelength and opsin. Adapted from Sharkey *et al.* (2020). c) Downstream targets of photoreceptors. All photoreceptor types project from the retina (gray) and make inhibitory connections (red lines) in the lamina (blue) or medulla (pink). R7 and R8 segregate by ommatidium type and synapse onto Dm9 neurons in the medulla, which feedback presynaptically to mediate color opponency. Dm8 and Tm5c are known to mediate spectral preference behavior. Black lines indicate excitatory connections.

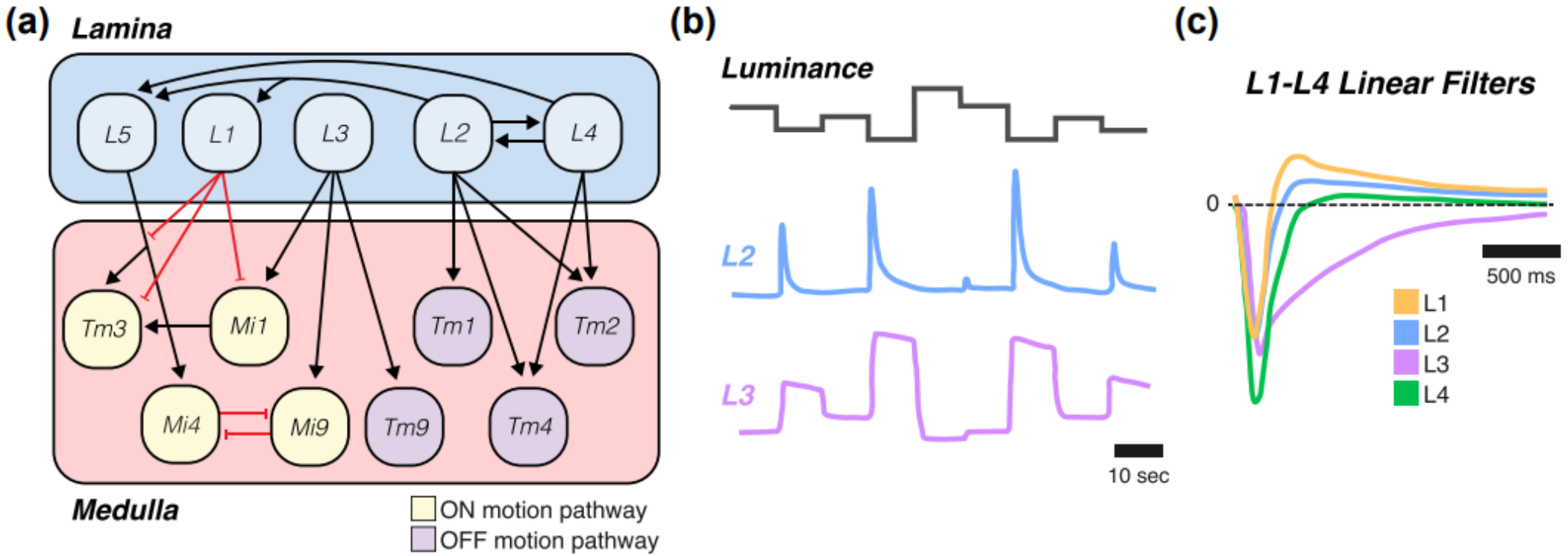

Fig. 4. Contrast and luminance representation in the lamina. a) Wiring diagram of the ON motion (yellow) and OFF motion (purple) pathways in the lamina and medulla. ON/OFF here refers only to whether a neuron is upstream of the ON or OFF motion detectors (T4 or T5) and does not necessarily mean that the neuron itself is ON or OFF selective. Colors as in Fig. 3c. b) Schematic plots of L2 (blue) and L3 (purple) responses to changes in luminance. L2 responds only to decreases in luminance (OFF contrast), while L3 shows sustained OFF activity. Adapted from Ketkar *et al.* (2020). c) Temporal filters for L1–L4. L1 (orange), L2 (blue), and L4 (green) are biphasic and are therefore contrast selective. L3 (purple) is monophasic and is therefore luminance selective. Dashed line indicates the vertical position where filter strength is 0. Adapted from Clark *et al.* (2011) and Silies *et al.* (2013).

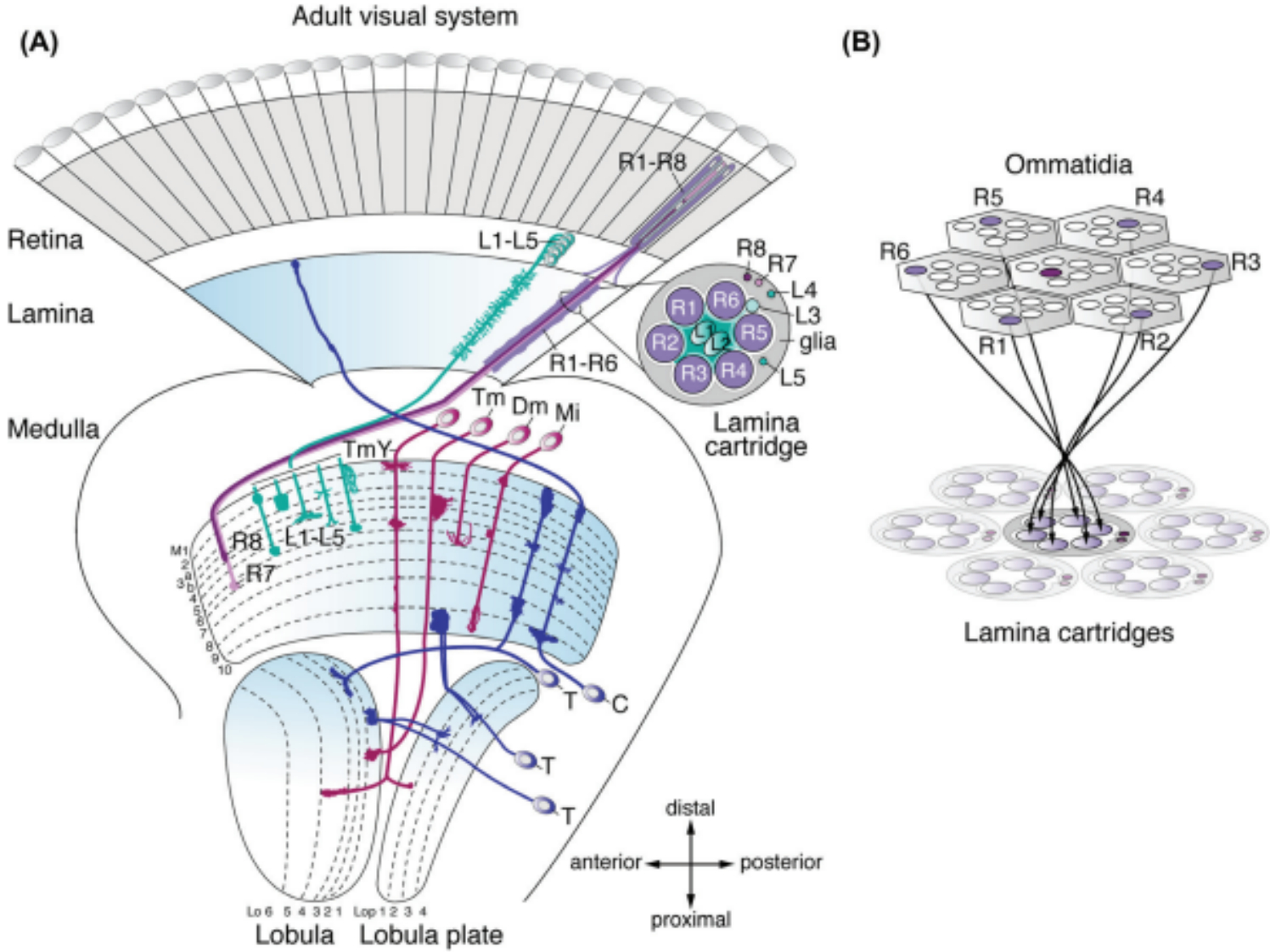

Figure 1. Architecture of the adult *Drosophila* visual system. (**A**) The optic lobe consists of the lamina, medulla, lobula plate, and lobula. The illustration shows a subset of neuron subtypes and their retinotopic projections. R1–R6 cells extend axons from the retina into the lamina, where they connect with lamina neurons L1–L3 in cartridges. Axons of R8 and R7 cells and lamina neurons L1–L5 terminate in one or more of ten medulla neuropil layers (M1–M10). Transmedullary neurons (Tm and TmY) project from the medulla to subsets of six lobula (Lo) and four lobula plate (Lop) neuropil layers. Distal medulla (Dm) neurons innervate several columns in upper medulla layers. Medulla intrinsic (Mi) neurons connect distal and proximal layers. C neurons extend branches into the medulla and lamina. T neurons connect the lobula or lobula plate and medulla, or lobula and lobula plate. (**B**) R1–R6 axons innervate lamina cartridges following the neural superposition principle.

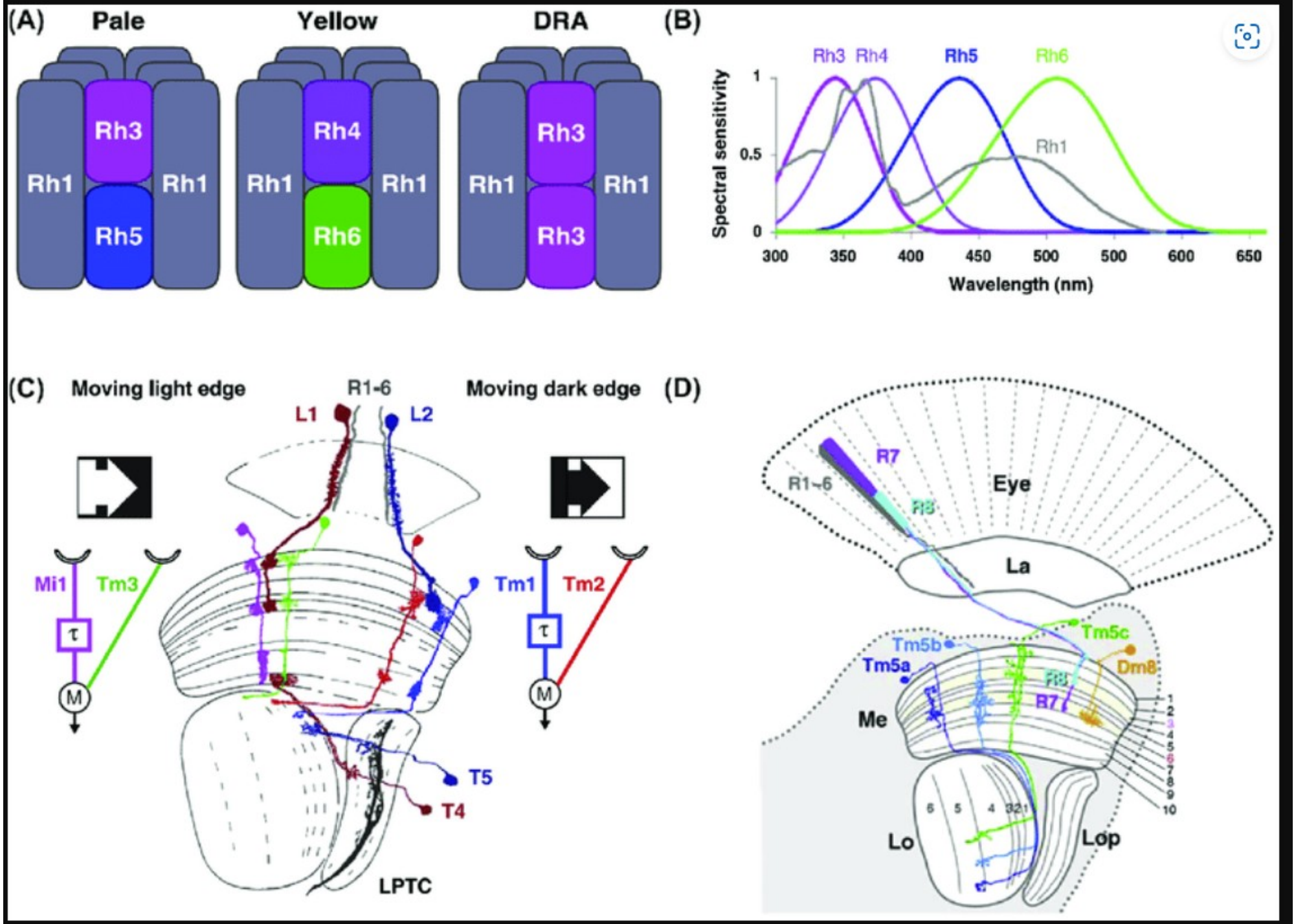
(A)
Pale
Yellow
DRA
Rh1
Rh3
Rh5
Rh4
Rh6
(B)
Rh3 Rh4
Rh5
Rh6
Rh1
Spectral sensitivity
1
0.5
0
300 350 400 450 500 500 600 650
Wavelength (nm)
(C)
Moving light edge
R1-6
Moving dark edge
L1
L2
Mi1
Tm3
Tm1
Tm2
τ
M
T5
T4
LPTC
(D)
R7
R1-6
Eye
R8
La
Tm5c
Tm5b
Tm5a
Dm8
R8
R7
Me
1
2
3
4
5
6
7
8
9
10
6 5 4 3 2 1
Lo
Lop

Table 1. Response properties of retina and lamina neuron types.

Cell type	ON response	OFF response	Temporal properties	Feature selectivity	Role in motion detection	Neurotransmitter
R1–R6	+	–	Fast, monophasic	—	ON and OFF motion	Hist
L1	–	+	Fast, biphasic	Contrast and luminance	ON motion and some OFF motion	Glu
L2	–	+	Fast, biphasic	Contrast	OFF motion and some ON motion	ACh
L3	–	+	Slow, monophasic	Luminance	ON and OFF motion in low-light contexts	ACh
L4	–	+	Fast, biphasic	—	—	ACh
L5	+	–	Fast, biphasic	—	—	ACh

For each cell type, the response to ON and OFF stimuli is shown, along with known temporal response properties, feature selectivity, and neurotransmitter type. For ON and OFF responses, "+" indicates depolarization, while "–" indicates hyperpolarization. "Role in motion detection" refers to demonstrated behavioral effects. Hist, histamine; Glu, glutamate; ACh, acetylcholine.

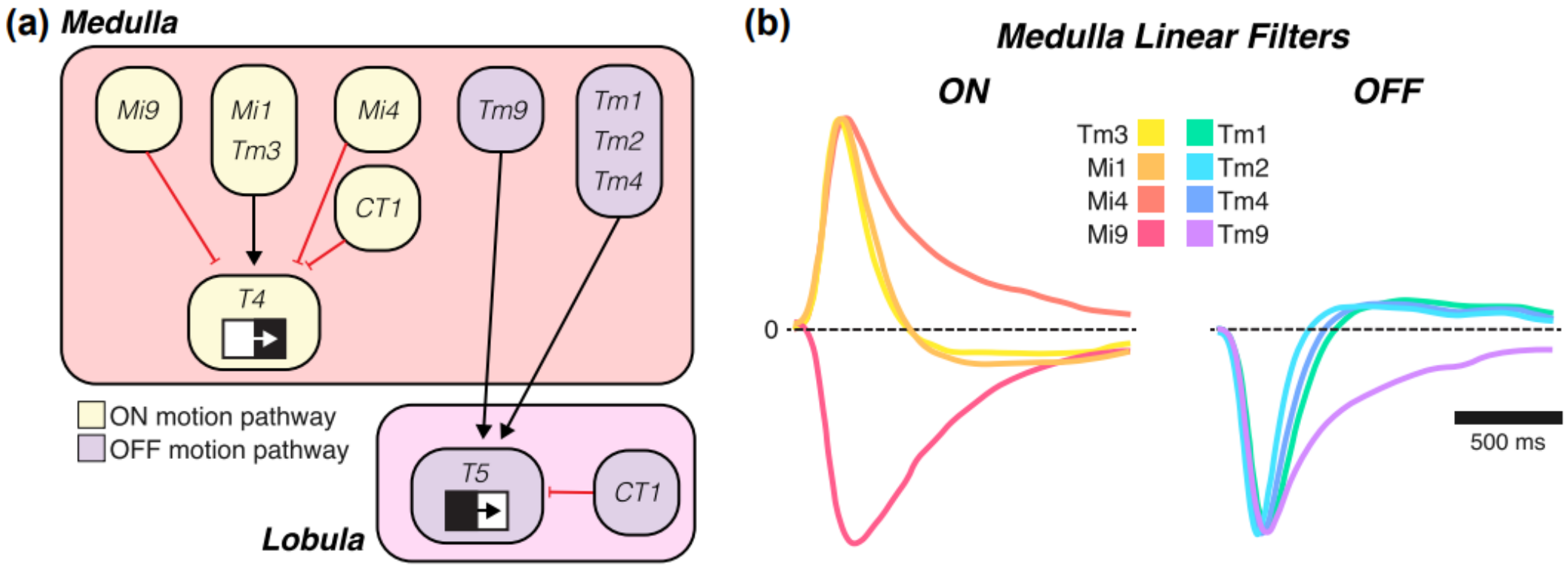

Fig. 5. Inputs to the T4/T5 motion detector. a) Wiring diagram of the ON motion (yellow) and OFF motion (purple) pathways in the medulla and lobula. ON/OFF here refers only to whether a neuron is upstream of the ON or OFF motion detectors (T4 or T5) and does not necessarily mean that the neuron itself is ON or OFF selective. Each CT1 terminal functions independently, and the cell as a whole contributes to both ON and OFF motion. The spatial arrangement of inputs represents their relative anatomical positioning, with the leading edge on the left. b) Temporal filters for the ON (left) and OFF (right) motion pathways. Mi1 and Tm1–Tm4 are more biphasic, whereas Mi4, Mi9, and Tm9 are slower and more monophasic. Mi9 responds negatively to ON stimuli, unlike the rest of the ON motion pathway inputs. Plotting conventions as in Fig. 4c. Adapted from Arenz *et al.* (2017).

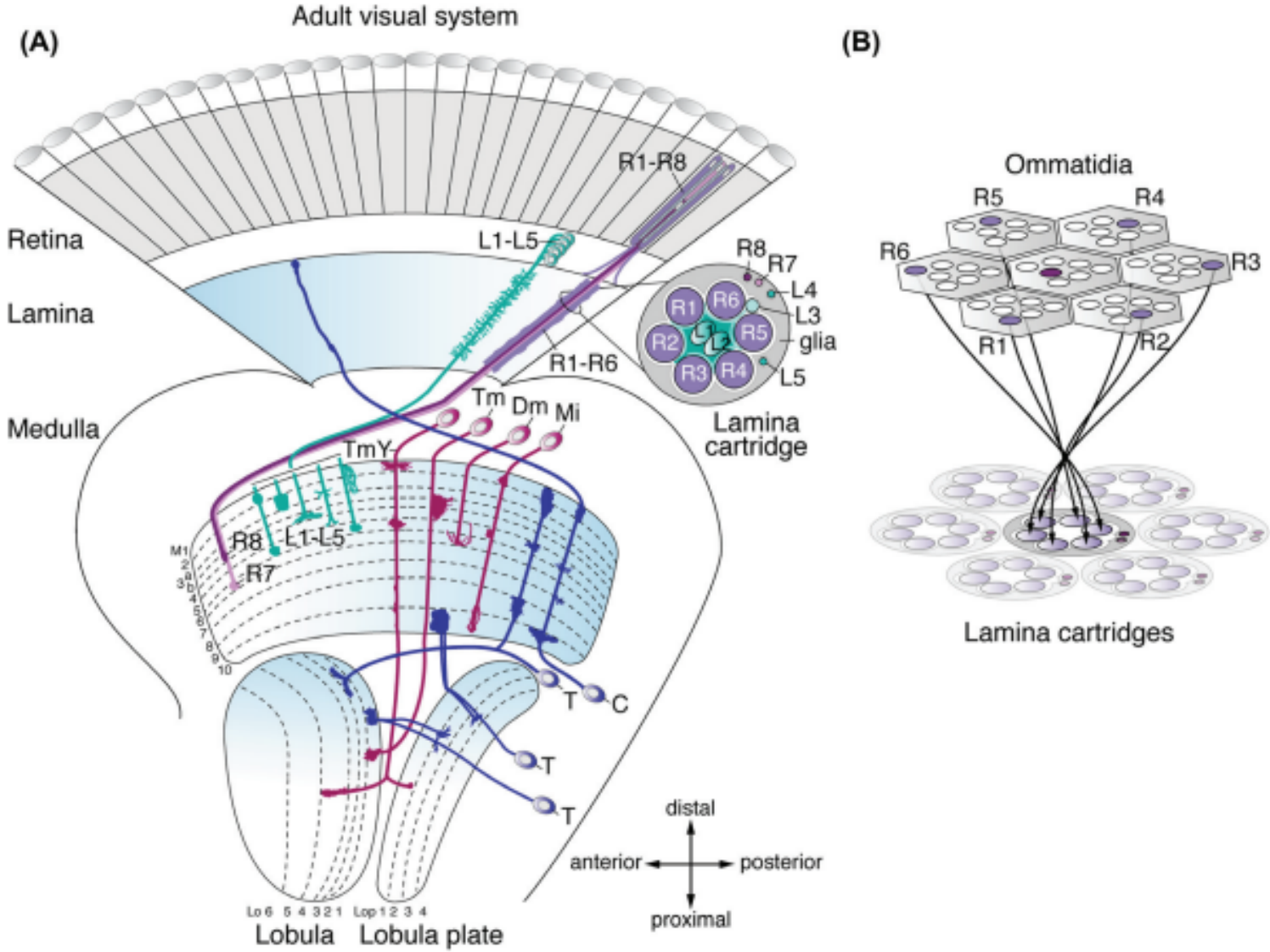

Figure 1. Architecture of the adult *Drosophila* visual system. (**A**) The optic lobe consists of the lamina, medulla, lobula plate, and lobula. The illustration shows a subset of neuron subtypes and their retinotopic projections. R1–R6 cells extend axons from the retina into the lamina, where they connect with lamina neurons L1–L3 in cartridges. Axons of R8 and R7 cells and lamina neurons L1–L5 terminate in one or more of ten medulla neuropil layers (M1–M10). Transmedullary neurons (Tm and TmY) project from the medulla to subsets of six lobula (Lo) and four lobula plate (Lop) neuropil layers. Distal medulla (Dm) neurons innervate several columns in upper medulla layers. Medulla intrinsic (Mi) neurons connect distal and proximal layers. C neurons extend branches into the medulla and lamina. T neurons connect the lobula or lobula plate and medulla, or lobula and lobula plate. (**B**) R1–R6 axons innervate lamina cartridges following the neural superposition principle.

Table 2. Response properties of medulla cell types.

Cell type	Temporal properties	Feature selectivity	Neurotransmitter	Output	Position of output
Mi1	Fast, biphasic	ON selective	ACh	T4	Center
Mi4	Slow, monophasic	ON selective	GABA	T4	Trailing edge
Mi9	Slow, monophasic	OFF selective	Glu	T4	Leading edge
Tm3	Fast, biphasic	ON selective	ACh	T4	Center
CT1 (med)	Fast, biphasic	ON selective	GABA	T4	Trailing edge
Tm1	Fast, biphasic	OFF selective	ACh	T5	Center
Tm2	Fast, biphasic	OFF selective (with ON information)	ACh	T5	Center
Tm4	Fast, biphasic	OFF selective	ACh	T5	Center
Tm9	Slow, monophasic	OFF selective (with ON information)	ACh	T5	Leading edge
CT1 (lob)	Fast, biphasic	OFF selective (with ON information)	GABA	T5	Trailing edge
Dm8	Slow, monophasic	UV–green color opponent	Glu	Tm5c	—
Dm9	Slow, biphasic	UV + green color selective	Glu	R7/R8	—

For each cell type, temporal response properties, visual feature selectivity, neurotransmitter, and major postsynaptic partners are shown. For neurons connected to T4 or T5, the position of that cell's output onto the T4 or T5 arbor is also listed (see Fig. 5a). CT1 has 2 entries because its neurites in the medulla (med) and lobula (lob) show distinct feature selectivity and connect with different postsynaptic partners. GABA, γ-aminobutyric acid; Glu, glutamate; ACh, acetylcholine.

Anterior and posterior central brain visual pathways

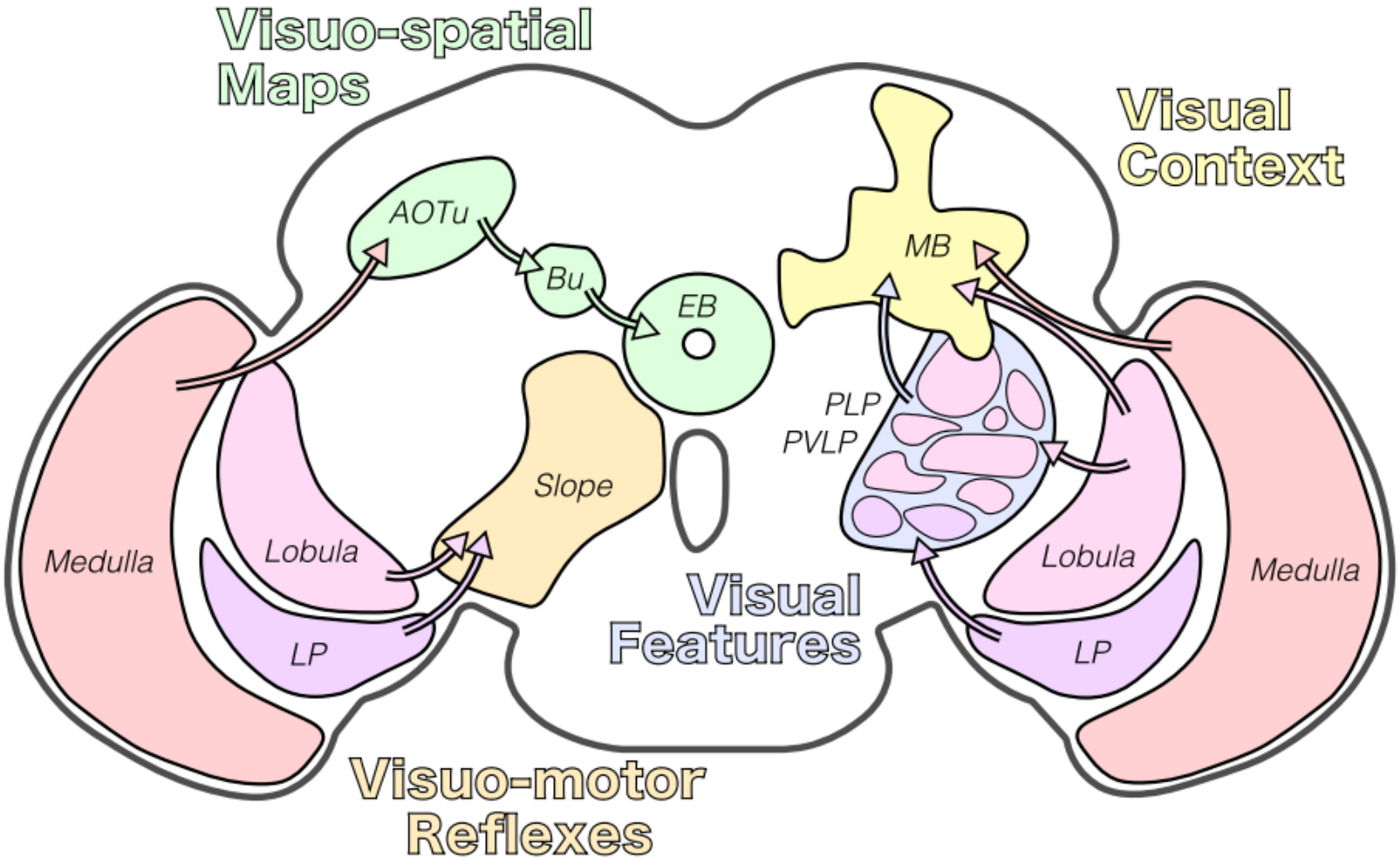

Fig. 6. Optic lobe signals are widely distributed across the brain. A simplified coronal section through the fly brain is shown, with major vision-responsive neuropil drawn in different colors. Outputs from the optic lobe (medulla, lobula, and lobula plate) to 4 central brain structures are highlighted: the anterior visual pathway (green), the mushroom body (yellow), the optic glomeruli (blue), and the posterior slope (orange). The categories of visual information represented in each of these regions are indicated by colored text.

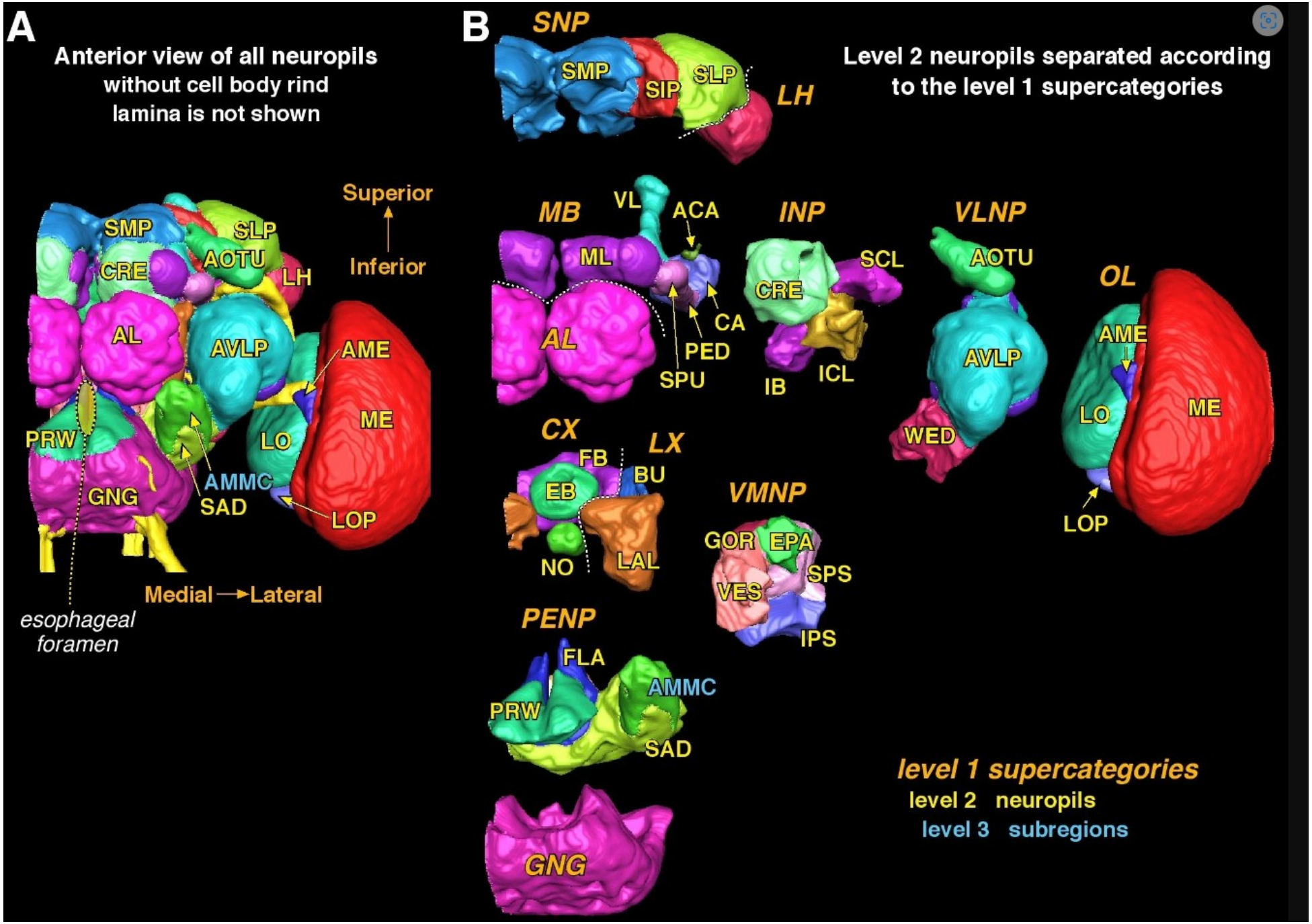
A
Anterior view of all neuropils
without cell body rind
lamina is not shown
Superior
Inferior
SMP
SLP
CRE
AOTU
LH
AL
AVLP
AME
ME
PRW
LO
AMMC
GNG
SAD
LOP
Medial → Lateral
esophageal foramen
B
SNP
SMP
SIP
SLP
LH
Level 2 neuropils separated according to the level 1 supercategories
MB
VL
ACA
ML
AL
SPU
PED
CA
INP
SCL
CRE
IB
ICL
VLNP
AOTU
AVLP
WED
OL
AME
LO
ME
LOP
CX
FB
EB
NO
LX
BU
LAL
VMNP
GOR
EPA
SPS
VES
IPS
PENP
FLA
AMMC
PRW
SAD
GNG
level 1 supercategories
level 2 neuropils
level 3 subregions

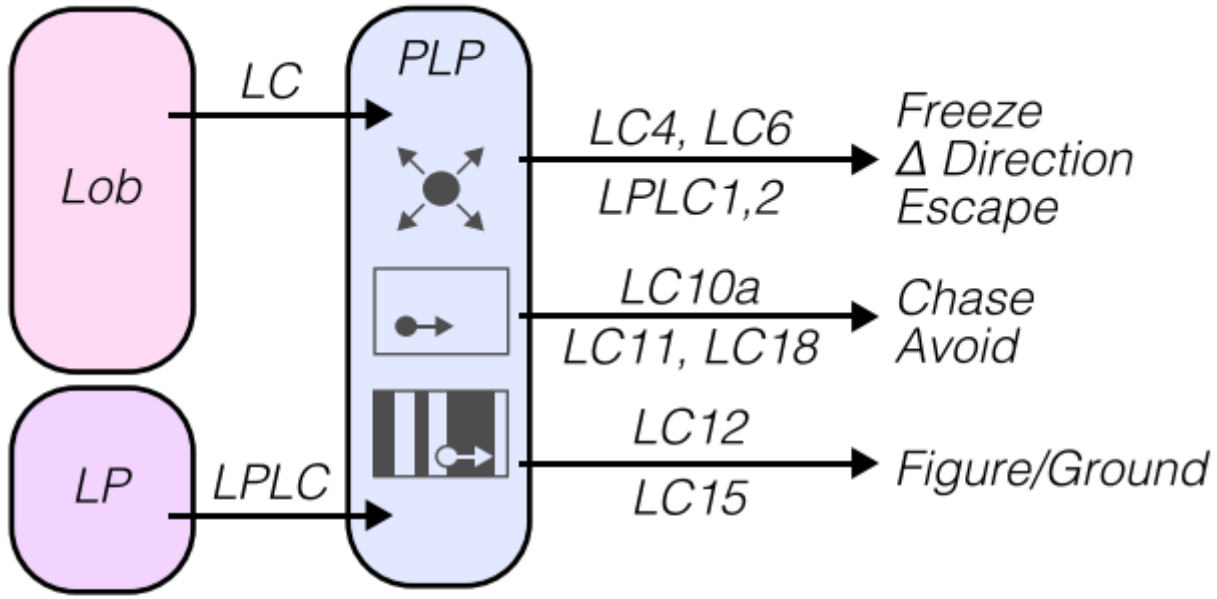

Fig. 7. LCs and LPLCs are selective for diverse and behaviorally relevant visual features. A simplified illustration of lobula (Lob, pink) and lobula plate (LP, purple) inputs to the posterior (ventro-)lateral protocerebrum (PLP, blue) is shown. Select PLP visual representations are also schematized: loom (top), small moving objects (middle), and figure/ground discrimination (bottom). LC and LPLC types associated with each representation are indicated.

Fast visual reflexes. Optomotor and escape responses.

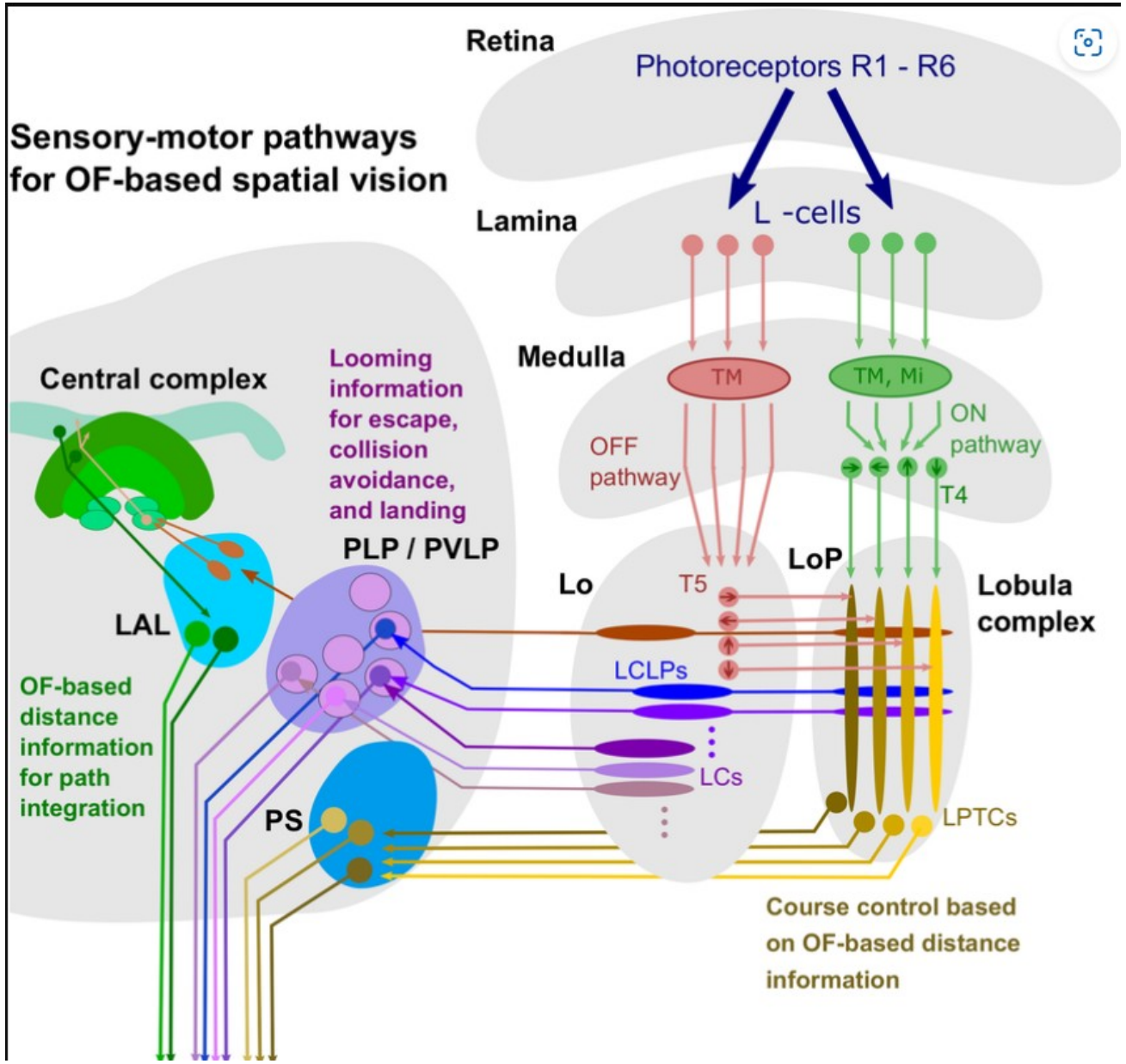

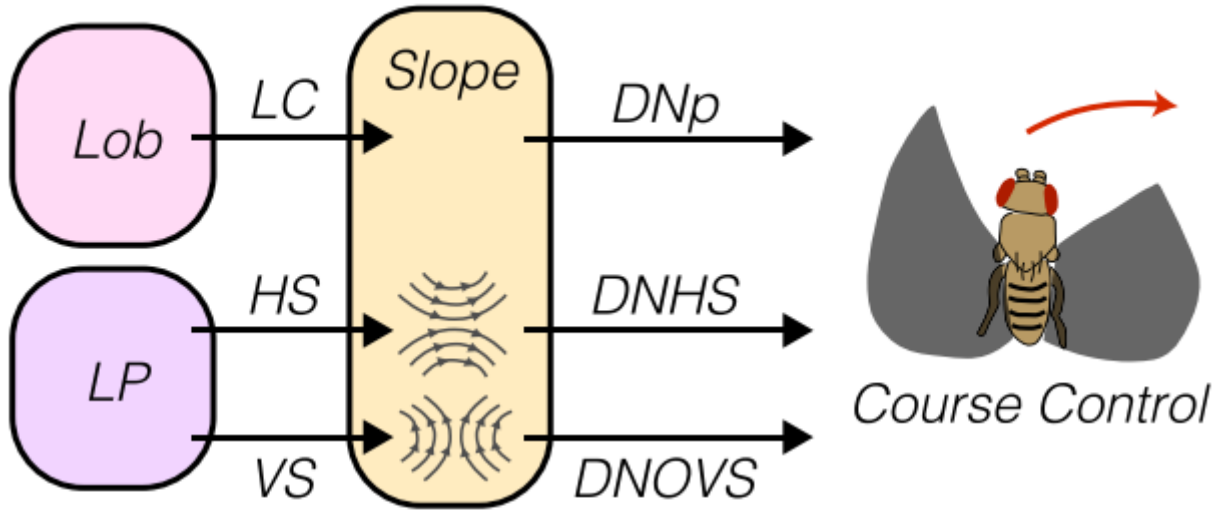

Fig. 10. Descending neuron control of vision-guided locomotion. A simplified illustration of visual input to select DN populations is shown, with arrows indicating connections between brain regions. Known cell types that form these connections are indicated. Lobula plate (purple) outputs from the horizontal and vertical systems (HS and VS) carry information about wide-field optic flow to course-controlling DNs in the posterior slope (orange). Some lobula (pink) outputs also connect to DNs in this region.

Giant fiber escape response pathway

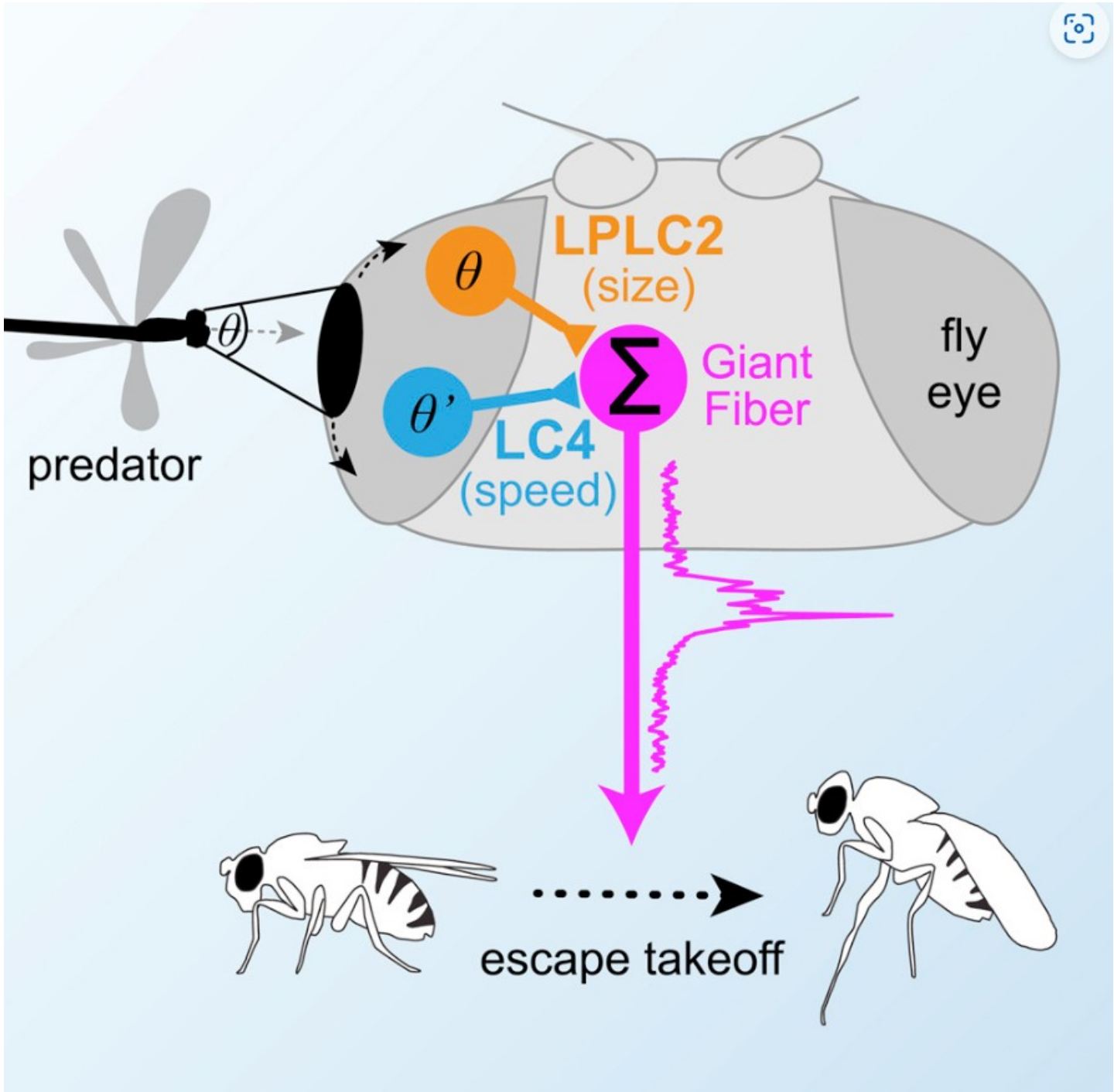

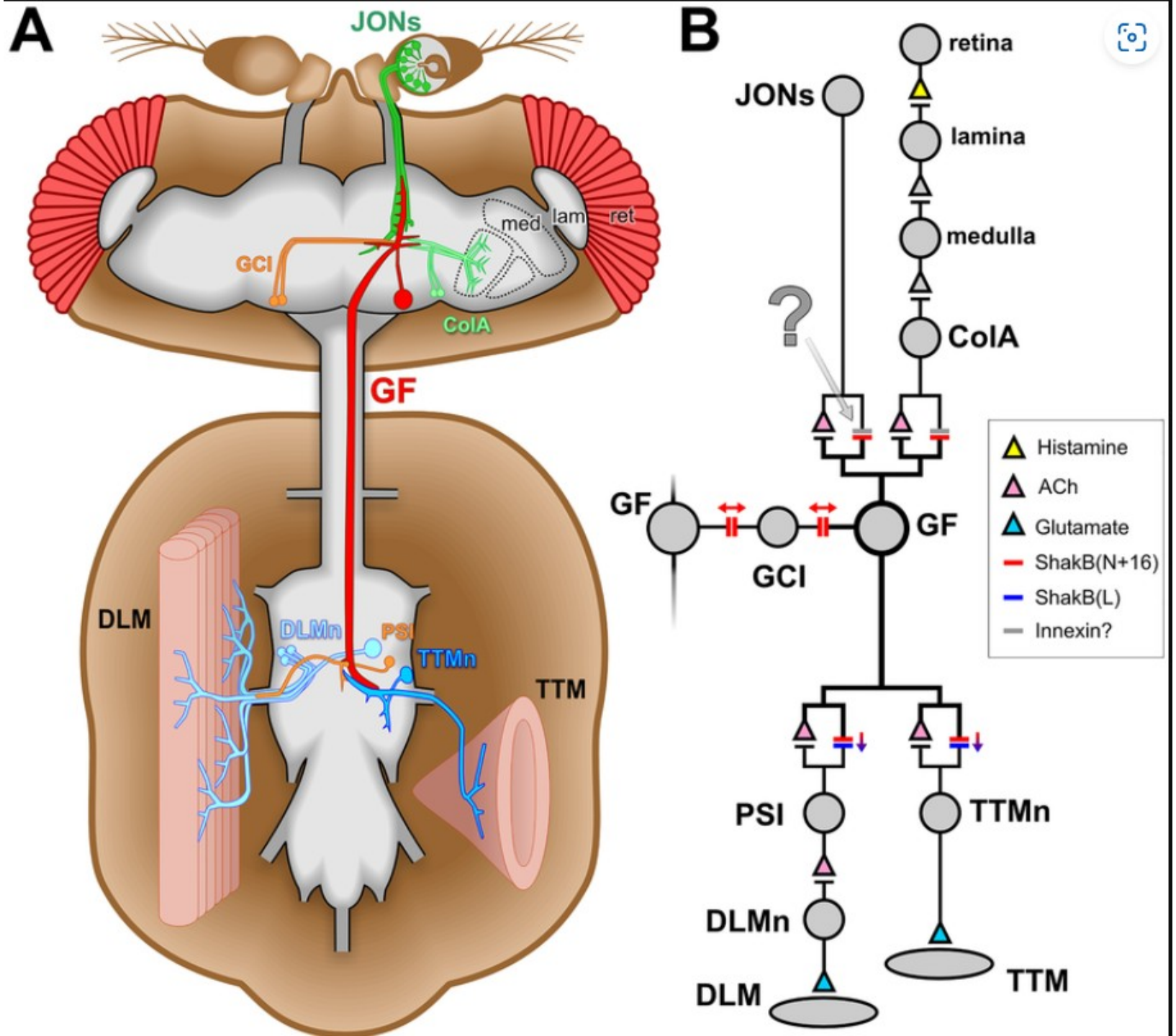
A
JONs
med
lam
ret
GCl
ColA
GF
DLM
DLMn
PSI
TTMn
TTM
B
retina
JONs
lamina
medulla
ColA
?
GF
GCl
GF
Histamine
ACh
Glutamate
ShakB(N+16)
ShakB(L)
Innexin?
PSI
TTMn
DLMn
DLM
TTM

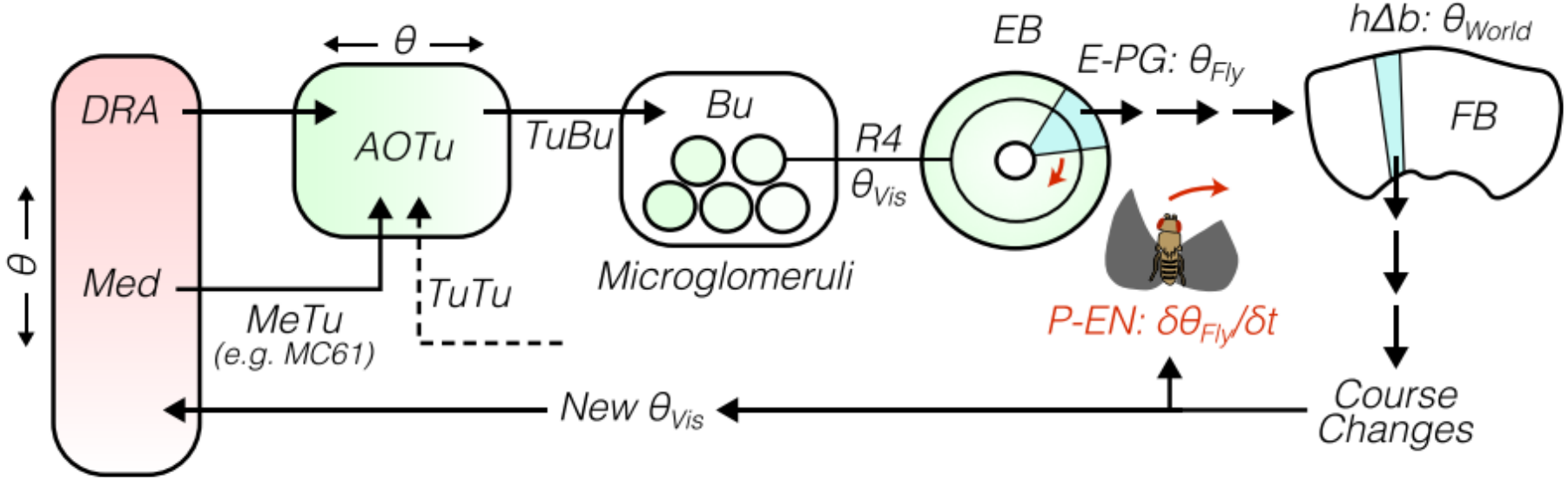

Fig. 8. The anterior visual pathway (AVP) and coordinate transformations in the central complex. A simplified illustration of the anterior visual pathway is shown, with color gradients indicating different portions of visual space. Arrows indicate connections between neuropil, and the cell types that make some of these connections are noted. The anterior visual pathway relays a visual object's position in retinal coordinates (θ_{Vis}), which are used to represent the fly's heading direction (θ_{Fly}) as a bump of activity in E-PG neurons of the ellipsoid body (EB). When the fly turns, changes to θ_{Fly} ($\delta\theta_{Fly}/\delta t$) are represented in P-EN neurons, which rotate the E-PG activity bump. In the fan-shaped body (FB), θ_{Fly} is transformed into allocentric coordinates (θ_{World}) in $h\Delta b$ neurons. See text for additional details. Med, medulla; DRA, dorsal rim area; AOTu, anterior optic tubercle; Bu, bulb.

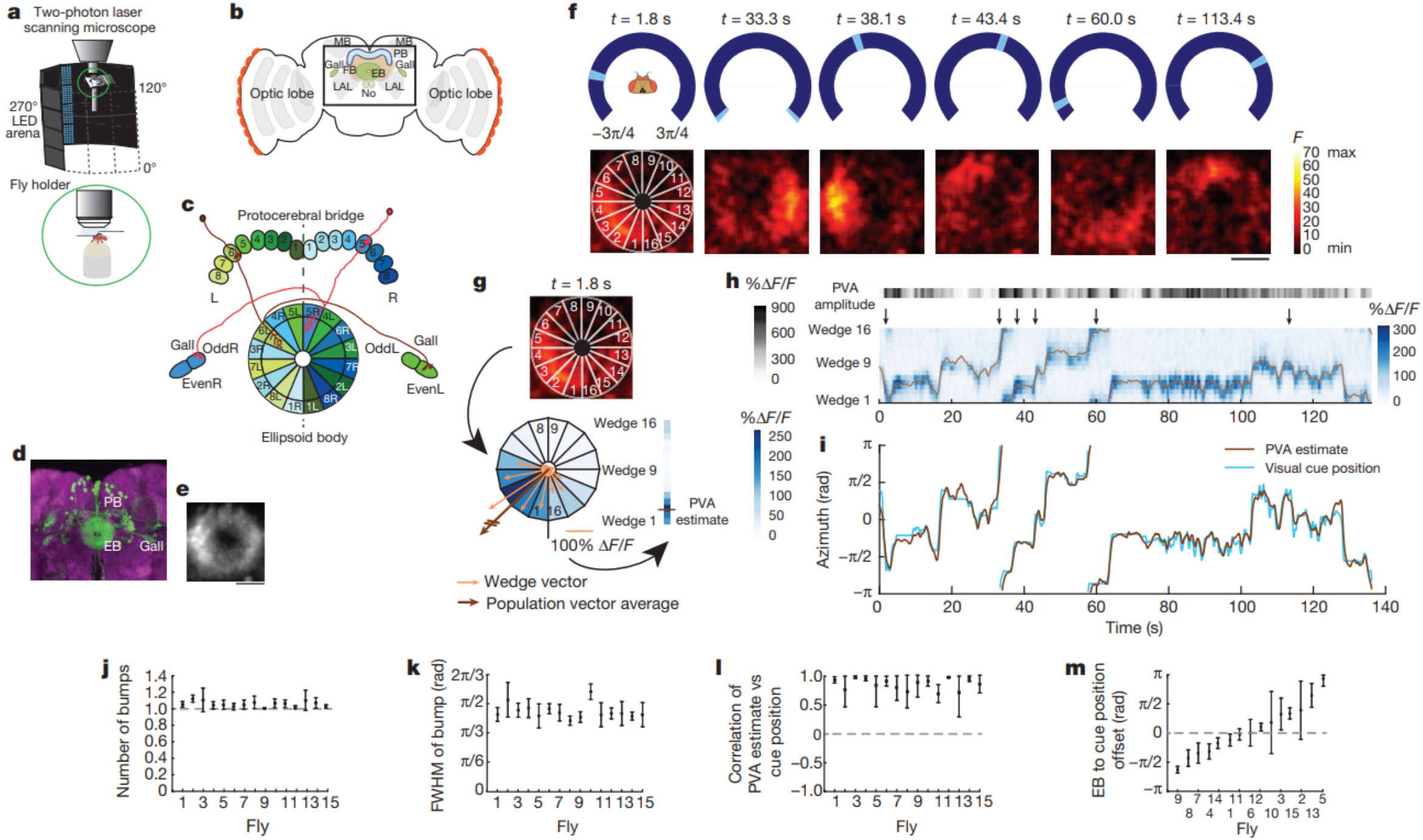
a
Two-photon laser scanning microscope
120°
270° LED arena
0°
Fly holder
b
MB
MB
PB
Gall
Gall
FB
EB
LAL
No
LAL
Optic lobe
Optic lobe
c
Protocerebral bridge
L
R
Gall
OddR
OddL
Gall
EvenR
EvenL
Ellipsoid body
d
PB
EB
Gall
e
f
t = 1.8 s
t = 33.3 s
t = 38.1 s
t = 43.4 s
t = 60.0 s
t = 113.4 s
−3π/4
3π/4
F
70 max
60
50
40
30
20
10
0 min
g
t = 1.8 s
Wedge 16
Wedge 9
Wedge 1
PVA estimate
100% ΔF/F
Wedge vector
Population vector average
h
%ΔF/F
900
600
300
0
PVA amplitude
Wedge 16
Wedge 9
Wedge 1
%ΔF/F
300
200
100
0
0
20
40
60
80
100
120
%ΔF/F
250
200
150
100
50
0
i
PVA estimate
Visual cue position
Azimuth (rad)
π
π/2
0
−π/2
−π
0
20
40
60
80
100
120
140
Time (s)
j
Number of bumps
1.4
1.2
1.0
0.8
0.6
0.4
0.2
0
1 3 5 7 9 11 13 15
Fly
k
FWHM of bump (rad)
2π/3
π/2
π/3
π/6
0
1 3 5 7 9 11 13 15
Fly
l
Correlation of PVA estimate vs cue position
1.0
0.5
0
−0.5
−1.0
1 3 5 7 9 11 13 15
Fly
m
EB to cue position offset (rad)
π
π/2
0
−π/2
−π
9 7 14 11 12 3 2 5
8 4 1 6 10 15 13
Fly

Figure 1 | Ellipsoid body activity tracks azimuth of visual cue. **a**, Schematic of setup. Inset, close-up of fly on air-supported ball (modified from ref. 20). **b**, Schematic of fly central brain and CX: ellipsoid body (EB), fan-shaped body (FB), protocerebral bridge (PB), paired noduli (NO), lateral accessory lobe (LAL) and gall (Gall). MB: mushroom body. **c**, Each EBw.s neuron receives inputs from an EB wedge and sends outputs to a corresponding PB column, and to the gall[24,26]. The PB has 18 columns[24], but EBw.s neurons only innervate the central 16. OddR, EvenR, OddL and EvenL, odd and even PB columns, right and left side of brain, respectively. **d**, GFP-labelled EBw.s neurons in a brain counterstained with nc82 (maximum intensity projection (MIP), reproduced with permission from Janelia FlyLight Image Database[23]). **e**, MIP of two-photon imaging stack (5 frames, 5 μm apart, see Methods) showing EB processes of GCaMP6f-labelled EBw.s neurons. **f**, Top, closed-loop walking with a vertical stripe. Bottom, EBw.s activity is measured in 16 regions of interest (ROIs). Sample frames from calcium imaging time series (Fly 15) showing MIP of EB activity bump (see Methods) as fly rotates visual cue around arena (top). *F*, fluorescence intensity (arbitrary units). Arrows near top of **h** indicate frame times. **g**, Steps to compute PVA based on EBw.s population activity. EB is unwrapped from Wedge 1 to Wedge 16 to display population time series in **h**. Superimposed is PVA estimate that incorporates trial-specific offset (**m**; see Methods). **h**, EBw.s fluorescence transients during a single trial (same trial as **f**). Colour scale at right. Superimposed brown line indicates PVA estimate of angular orientation of visual cue. Top, horizontal greyscale stripe shows PVA amplitude; intensity scale at left. **i**, PVA estimate of angular orientation plotted against actual orientation of visual cue (see Methods). **j**, Mean and standard deviation (s.d.) of number of activity bumps in EBw.s population activity across trials for each of 15 flies (see Methods). **k**, Mean and s.d. of full width at half maximum (FWHM) of activity bump across trials and flies (see Methods). **l**, Mean and s.d. of correlation between PVA estimate and actual orientation (pattern position) (see Methods). **m**, Mean and s.d. of angular offsets between PVA position and pattern position (see Methods, Extended Data Fig. 2e, f). All scale bars, 20 μm.

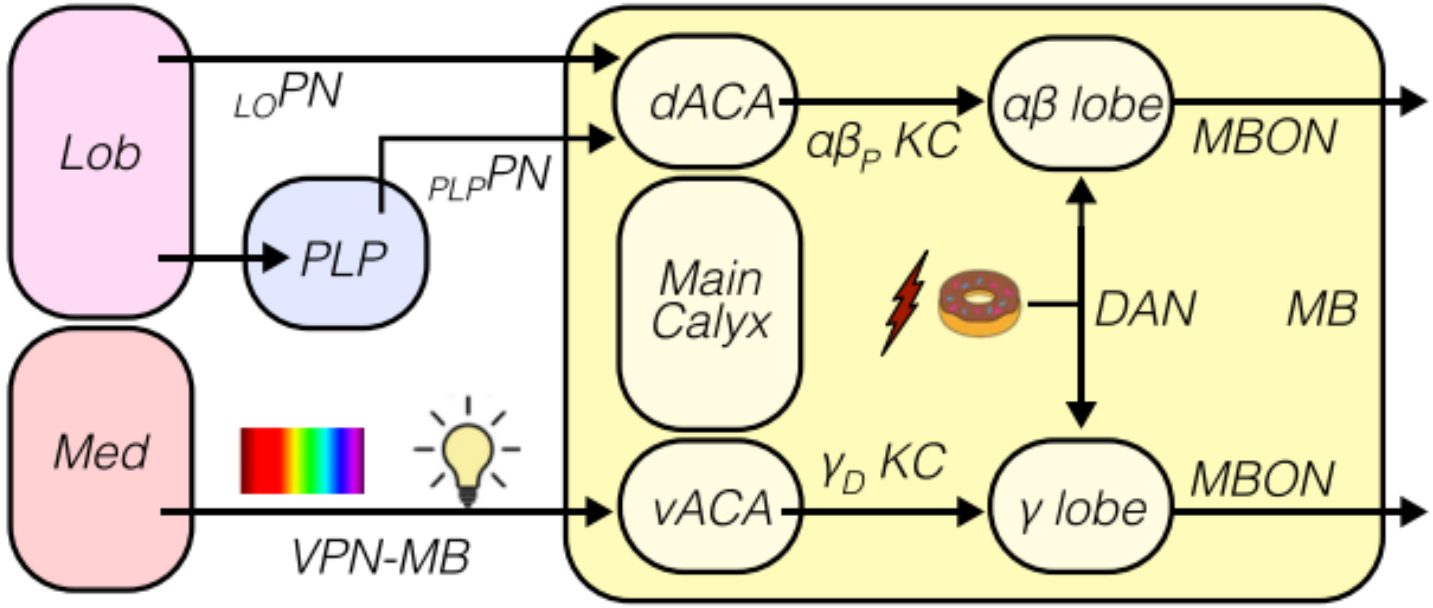

Fig. 9. Color and luminance are contextual cues for visual learning in the mushroom body (MB, yellow). Lobula (pink) and medulla (red) inputs to the mushroom body are schematized, with arrows indicating connections between brain regions. Known cell types that form these connections are indicated. Medulla outputs carry information about the spectral content and brightness of ambient light to the ventral accessory calyx (vACA), while lobula outputs directly and indirectly connect to the dorsal accessory calyx (dACA). Visual inputs do not innervate the main calyx, where olfactory information enters the mushroom body. Distinct Kenyon cell (KC) populations carry information from the accessory calyces to mushroom body output neurons (MBONs), and dopaminergic neurons (DANs) modify the strength of this connection based on reward or punishment, facilitating associative learning.

OXFORD GENETICS

GENETICS, 2023, 224(2), iyad064
https://doi.org/10.1093/genetics/iyad064
Advance Access Publication Date: 2 May 2023
FlyBook

Visual processing in the fly, from photoreceptors to behavior

Timothy A. Currier,† Michelle M. Pang,† Thomas R. Clandinin*

Department of Neurobiology, Stanford University School of Medicine, Stanford, CA 94305, USA

*Corresponding author: Department of Neurobiology, Stanford University School of Medicine, 299 W. Campus Drive, Stanford, CA 94305, USA. Email: trc@stanford.edu
†These authors contributed equally.

Abstract

Originally a genetic model organism, the experimental use of *Drosophila melanogaster* has grown to include quantitative behavioral analyses, sophisticated perturbations of neuronal function, and detailed sensory physiology. A highlight of these developments can be seen in the context of vision, where pioneering studies have uncovered fundamental and generalizable principles of sensory processing. Here we begin with an overview of vision-guided behaviors and common methods for probing visual circuits. We then outline the anatomy and physiology of brain regions involved in visual processing, beginning at the sensory periphery and ending with descending motor control. Areas of focus include contrast and motion detection in the optic lobe, circuits for visual feature selectivity, computations in support of spatial navigation, and contextual associative learning. Finally, we look to the future of fly visual neuroscience and discuss promising topics for further study.

Keywords: neuroscience, vision, anatomy, physiology, computation, behavior, navigation, learning, FlyBook

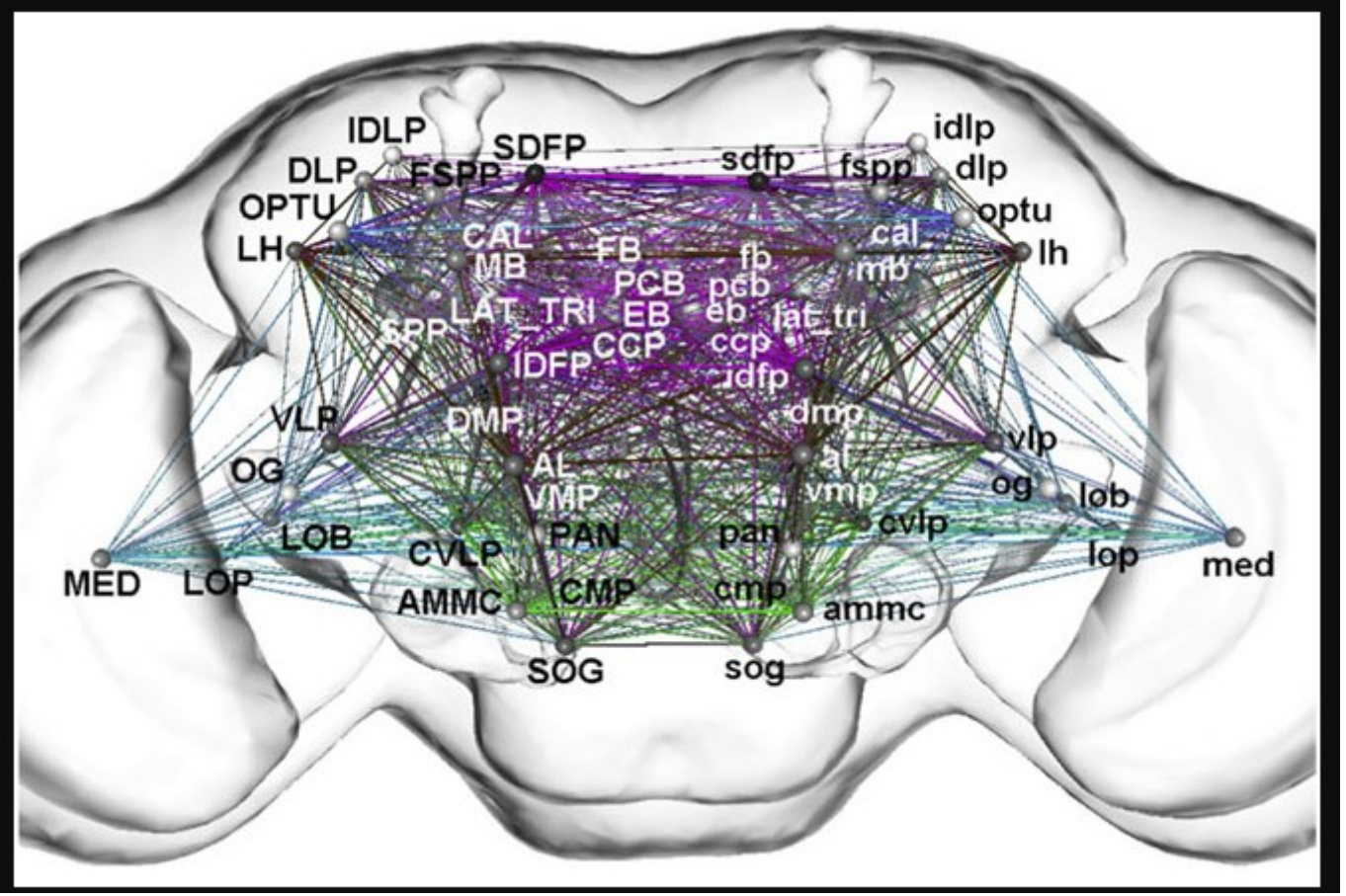
lDLP
SDFP
DLP
FSPP
OPTU
LH
CAL
FB
MB
PCB
LAT
TRI
EB
SPP
CCP
lDFP
VLP
DMP
AL
OG
VMP
LOB
PAN
CVLP
MED
LOP
AMMC
CMP
SOG
idlp
sdfp
fspp
dlp
optu
cal
lh
mb
fb
pcb
lat
tri
eb
ccp
idfp
dmp
vlp
al
og
vmp
lob
cvlp
lop
med
pan
cmp
ammc
sog

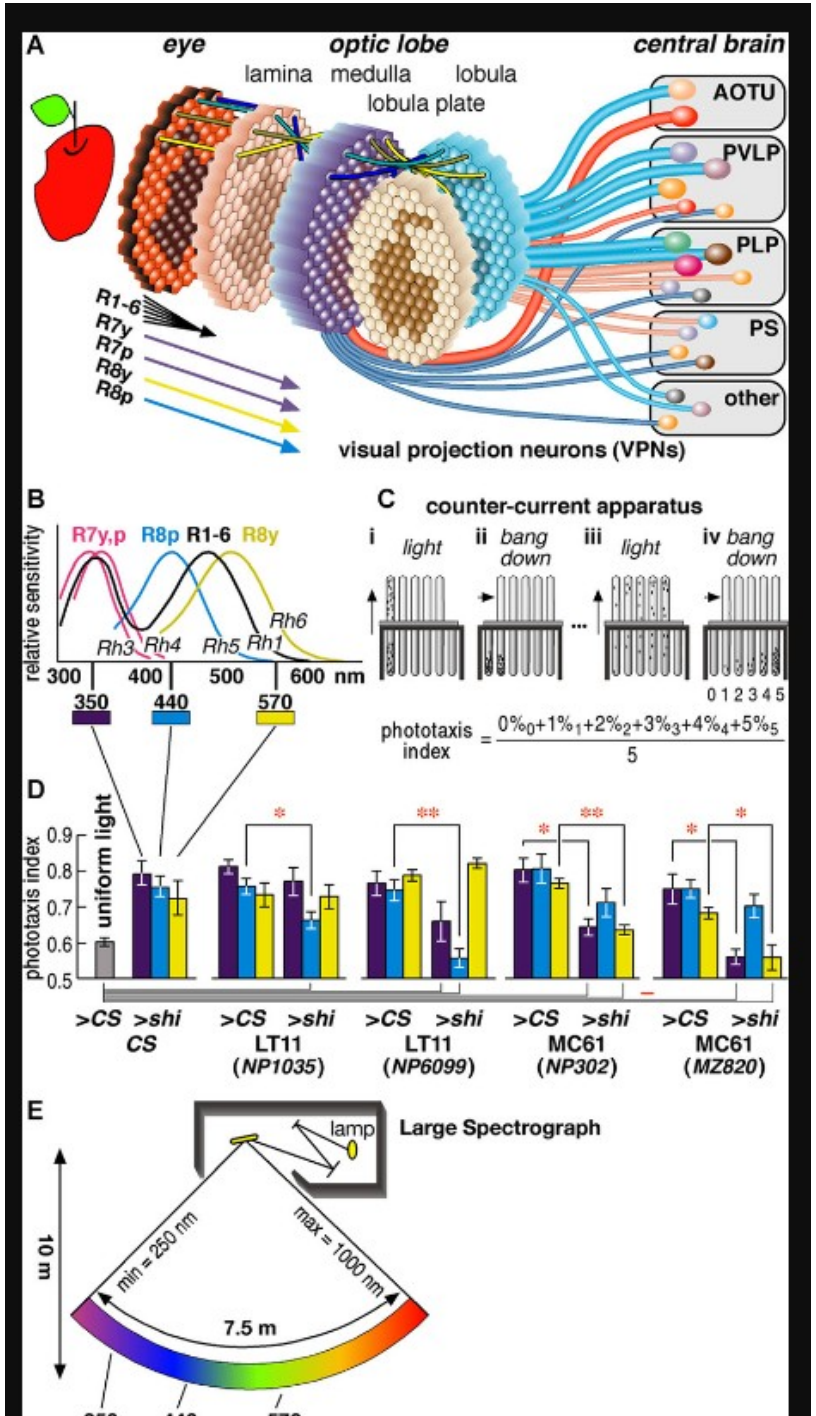

FIGURE 1 | *Drosophila* visual system and phototaxis assay. (A) Schematic diagram of the *Drosophila* visual system. Photoreceptors project from about 750 ommatidia of the retina to as many retinotopic columns (visual cartridges) in the four nested neuropils of the optic lobe. Relay interneurons project each retinotopic level onto the next (indicated by four colored lines on top of each neuropil). Hexagons with the projected images of an apple schematize the distribution of retinotopic visual cartridges and the relayed visual field. Cylindrical lines represent the visual projection neurons (VPNs) that connect the lower visual centers in the optic lobe to higher visual centers in the central brain (Otsuna and Ito, 2006). They terminate in the anterior optic tubercle (AOTU), posterior ventrolateral protocerebrum (PVLP), posterior lateral protocerebrum (PLP), posterior

FIGURE 1 | Continued
wild-type *CS* flies in the apparatus lit completely uniformly with white lamp (as negative control) and of the *CS* flies and GAL4 driver lines crossed with either *CS* (>*CS*, as positive control) or UAS-*shi*^{ts1} (>*shi*) towards specific wavelengths of light (at 30°C). Mean ± SEM of three independent measurements with different sets of flies were shown. Statistical significance of differences by *t*-test is indicated with * ($p < 0.05$) and ** ($p < 0.01$) below the abscissa indicates the cases that were not significantly different from the behavior under uniform light ($p > 0.05$). **(E)** Schematic diagram of the Okazaki Large Spectrograph (OLS).